Spatiotemporal cat: An exact classical field theory

P Cvitanović and H Liang

Center for Nonlinear Science, School of Physics, Georgia Institute of Technology, Atlanta, GA 30332-0430, USA

E-mail: predrag.cvitanovic@physics.gatech.edu

9 December 2019

Abstract.

While the global dynamics of an extended, spatiotemporally chaotic (or 'turbulent') system can be extraordinarily complex, the local dynamics, observed through small spatiotemporal finite windows, can be thought of as a visitation sequence through finite repertoires of finite patterns. To compute spatiotemporal expectation values of observables from the defining equations of such systems, one needs to know how often a given pattern occurs. Here we address this fundamental question by constructing a 'spatiotemporal cat', a classical d-dimensional spatiotemporal lattice field theory. In this field theory any spatiotemporal state is labeled by a unique d-dimensional lattice block of symbols from a finite alphabet, with any lattice state and its symbolic encoding related linearly. We show that the state of the system over a finite spatiotemporal region can be described uniquely and with exponentially increasing precision by finite blocks of such symbols, and that the likelihood of such state occurring is given by its linear spatiotemporal stability.

PACS numbers: 02.20.-a, 05.45.-a, 05.45.Jn, 47.27.ed

Submitted to: *Nonlinearity*

1. Introduction

While the technical novelty of this paper is in working out details of the spatiotemporal cat, an elegant, but very special model of many-particle dynamics (or discretization of a classical d-dimensional field theory), the vision that motivates it is much broader. We address here the long standing problem of how to describe, by means of discrete symbolic dynamics, the spatiotemporal chaos (or turbulence) in spatially extended, strongly nonlinear field theories.

Flows described by partial differential equations are in principle infinite dimensional, and, at first glance, turbulent dynamics that they exhibit might appear hopelessly complex. However, what is actually observed in experiments and simulations is that turbulence is dominated by repertoires of identifiable recurrent vortices, rolls, streaks and the like [50]. Dynamics on a low-dimensional chaotic attractor can be visualized

as a succession of near visitations to exact unstable periodic solutions of the equations of motion, interspersed by transient interludes [31]. In the same spirit, the long-term turbulent dynamics of spatially extended systems can be thought of as a sequence of visitations through the repertoire of admissible spatiotemporal patterns, each framed by a finite spatiotemporal window. The question we address here is: can states of a strongly nonlinear field theory be described by such repertoires of admissible patterns explored by turbulence? And if yes, what is the likelihood to observe any such pattern?

Such questions have been studied extensively for systems of small spatial extension, where the attractor dimension is relatively small [23, 27, 30, 61, 91]. However, going from spatially small to spatially infinite systems will require completely new tools. For small systems the long time dynamics can be thought of as motion of a point within an inertial manifold of a moderate dimension. A temporally chaotic system is exponentially unstable with time: double the time, and exponentially more periodic orbits are required to cover its strange attractor to the same accuracy. For large spatial extents, the complexity of the spatial shapes also needs to be taken into account; double the spatial extent in a given direction, and exponentially as many distinct spatiotemporal patterns will be required to describe the repertoire of system's shapes to the same accuracy. The systems whose temporal and spatial correlations decay sufficiently fast, and whose "physical" dimension [33, 42] grows with system size, are said to be "spatiotemporally chaotic." The observation that for spatiotemporally chaotic systems space and time should be considered on the same footing goes back to Politi and collaborators [39, 63, 64, 83] who, in their studies of propagation of spatiotemporal disturbances in extended systems, discovered that the spatial stability analysis can be combined with the temporal stability analysis.

> [2019-06-26 Predrag] Physical picture:
> Turbulence everywhere in space, with a range of length scales. Discretize into cells, with each box turbulent, and cells isotropically and homogenously coupled to their nearest neighbors [55].
> As a function of the strengths of cell-cell couplings, dynamics can exhibit rich phase-transitions structure [56]. In this paper we chose couplings such that the system is fully turbulent.
> Explain word "turbulence" as used here.
> Hamiltonan, so symplectic or area preserving. Cite the Hamiltonian zeta function from ChaosBook.

One way to capture the essential features of turbulent motions of a physical flow is offered by coupled map lattice models, in which the spacetime is coarsely discretized, with the dynamics of domains that capture important small-scale spatial structures modeled by discrete time maps (Poincaré sections of a single "particle" dynamics) attached to lattice sites, and the coupling to neighboring sites consistent with the translational and reflection symmetries of the problem. Here we shall follow this path by investigating the Gutkin and Osipov [47] d-dimensional coupled cat maps lattice ("spatiotemporal cat" for short, in what follows), which satisfiers the d-dimensional

lattice screened Poisson equation

$$(-\Box + s - 2d)\, x_z = m_z\,.$$

Spatiotemporal cat is built from the Anosov-Arnol'd-Sinai cat maps (modeling the Hamiltonian dynamics of individual "particles") at sites of a $(d-1)$-dimensional spatial lattice, linearly coupled to their nearest neighbors. The remarkable feature of the spatiotemporal cat is that its every solution X is uniquely encoded by a linear transformation to the corresponding finite alphabet d-dimensional symbol lattice state M, a spatiotemporal generalization of the linear code for temporal evolution of a single cat map, introduced in the beautiful 1987 paper by Percival and Vivaldi [76].

Within this model, a spatial-temporal window into system dynamics is provided by a finite block of symbols, and the central question is to understand which symbol blocks are admissible, and what is the likelihood of a given block's occurrence. It was already noted in [47] that two spatiotemporal orbits that sharing a same finite symbol block shadow each other exponentially well within the corresponding spatial-temporal window. This is the key property of hyperbolic spatiotemporal dynamics that we explore in detail in this paper. The linearity of the spatiotemporal cat enables us to go far analytically; standard crystallographic methods enable us to count spatiotemporally finite blocks, and give explicit formulas for the number of invariant d-torus solutions for blocks of any size.

2019-06-26 Predrag Currently the argument flow of [28] (this paper) is:

(i) Hamiltonian cat map
  (a) Percival-Vivaldi map
  (b) Adler-Weiss generating partition and transition graph

(ii) Lagrangian cat map
  (a) Hamiltonian, Lagrangian
  (b) screened Poisson equation

(iii) Periodic orbits theory of cat maps
  (a) orbit counting
  (b) Adler-Weiss zeta function of transition graph
  (c) Hamiltonian volume formula
  (d) Lagrangian Hessian
  (e) Hill's formula

(iv) Spatiotemporal cat (Predrag: I call it simply spatiotemporal cat, as it is not a "map")
  (a) time, space Laplacians $\to$ screened Poisson equation
  (b) Lagrangian
  (c) Hessian, reciprocal lattice, spectrum formula for volume

Although we can also get the Lagrangian cat map (**??**) from the linear code (11), we still need to write down the Lagrangian explicitly to define the Hessian matrix, $(H_n)_{ij} = \partial^2 L(\boldsymbol{x})/\partial x_i \partial x_j$. Then we can use the Hill's formula to show that the two counting methods are equivalent.

The paper is organized as follows: In section 2 we review the traditional cat map in its usual, Hamiltonian formulation, and construct an explicit generating (Adler-Weiss) partition of the cat map phase space, section 2.1. In section 3 we review the 'temporal cat', the Lagrangian reformulation of cat map. The periodic orbits theory of cat maps, section 4, can be developed in either formulation: both the Hamiltonian cat map periodic orbits counting (section 4.1) and the Lagrangian temporal cat periodic orbits counting (section 4.2) lead to the same topological zeta function, with the two formulations related by Hill's formula (section 4.3). A reader may skip Sections 2 to 4 on the first reading, as the paper proper starts with section 5.

In section 5 (after a brief review of the traditional coupled map lattices, section 5.1), we extend the temporal cat to the d-dimensional spatiotemporal cat, section 5.2. In section 5.3 we show that the system admits a natural d-dimensional symbolic code with a finite alphabet, and then study finite spatiotemporal symbol blocks.

Section 6 *Invariant tori in d-dimensional spatiotemporal cat* introduces the method of finding eigenmodes in d-dimensional spatiotemporal cat.

In section 6 we use these results to construct sets of spatiotemporal invariant 2-tori that partially shadow each other.

The new results follow from our determination of phase space generating partitions generated by the iterations of the cat map, for different integer values of the stretching parameter s.

The results are summarized and some open questions discussed in the section 7.

In Appendix A we collect the symbolic dynamics definitions needed throughout the paper.

Implementing this program requires several tools not standard in dynamicist's tool box: lattice Green's functions, new kinds of determinants, new relations between propagation of temporal vs. spatial disturbances; some of these are derived in XXX eq. s:Green.

Before turning to the spatially infinite field theory in section 5, it is instructive to motivate our formulation of the "spatiotemporal cat" by a discussion of the traditional cat map (a 1-dimensional temporal lattice) in its Hamiltonian and Lagrangian formulations.

2. Life of a single Hamiltonian cat

We start with a brief review of the physical origin of cat maps. Hamiltonian (area-preserving, symplectic) 1-degree of freedom maps that describe kicked rotors subject to discrete time sequences of angle-dependent impulses $P(q_t)$, $t \in \mathbb{Z}$,

$$q_{t+1} = q_t + p_{t+1} \qquad \mod 1, \tag{1}$$

$$p_{t+1} = p_t + P(q_t)\,, \tag{2}$$

play important role in the theory of chaos in Hamiltonian systems, from the Taylor, Chirikov and Greene standard map [22, 66], to the temporally evolving cat map reviewed here. Here $2\pi q$ is the angle of the rotor, p is the momentum conjugate to the angular coordinate q, angular pulse $P(q) = P(q+1)$ is periodic with period 1, and the time step has been set to $\Delta t = 1$. Eq. (1) says that in one time step Δt the configuration trajectory starting at q_t reaches $q_{t+1} = q_t + p_{t+1}\Delta t$, and (2) says that at each kick the angular momentum p_t is accelerated to p_{t+1} by the force $P(q_t)\Delta t$. As the values of q differing by integers are identified, and the momentum p is unbounded, the phase space is a cylinder. However, one can analyze the dynamics just as well on the compactified phase space, with the momentum wrapped around a circle, i.e., adding $\mod 1$ to (2). Now the dynamics is a toral automorphism acting on a $(0,1]\times(0,1]$ phase space square of unit area, with the opposite edges identified.

The simplest example of (1,2) is a rotor subject to a force $P(q) = Kq$ linear in the displacement q. The $\mod 1$ added to (2) makes this a discontinuous 'sawtooth', unless K is an integer. In that case the map (1,2) is known as a Continuous Automorphism of the Torus, or a *cat map* [5], a linear area-preserving map on the unit 2-torus phase space, with coordinates $x = (q_t, p_t)$ interpreted as the angular position variable and its conjugate momentum at time instant t. Explicitly:

$$\begin{pmatrix} q_{t+1} \\ p_{t+1} \end{pmatrix} = A \begin{pmatrix} q_t \\ p_t \end{pmatrix} \mod 1\,, \qquad A = \begin{pmatrix} a & c \\ d & b \end{pmatrix}\,, \tag{3}$$

where a, b, c, d are integers whose precise values do not matter, as long as $\det A = 1$, so that the map is area preserving.

A cat map (3) is a fully chaotic Hamiltonian dynamical system if its stability multipliers $(\Lambda\,,\ \Lambda^{-1})$, where

$$\Lambda = e^{\lambda} = (s + \sqrt{(s-2)(s+2)})/2\,, \qquad s = \mathrm{tr}\, A = \Lambda + \Lambda^{-1}\,, \tag{4}$$

are real, with a positive Lyapunov exponent $\lambda > 0$. The eigenvalues are functions of a single stretching parameter s, and for $|s| > 2$ the map is chaotic. All cat maps with the same s are equivalent up to a similarity transformation, i.e., coordinatization of the unit torus, so it suffices to work out a single convenient example (6), as we shall do here.

We shall refer here to the least unstable of the cat maps (3), with $s = 3$, as the 'Arnol'd cat map' [5, 32], and to maps with integer $s \geq 3$ as 'cat maps'. Cat maps have been extensively analyzed as particularly simple examples of chaotic Hamiltonian dynamics. They exhibit ergodicity, mixing, exponential sensitivity to variation of the

initial conditions (the positivity of the Lyapunov exponent), and the positivity of the Kolmogorov-Sinai entropy [90]. Detailed understanding of dynamics of cat maps is important also for the much richer world of nonlinear hyperbolic toral automorphisms, see [24, 38, 89] for examples.

2.1. Linear code partition of the cat map phase space

The discrete time Hamilton's equations (1,2) induce temporal evolution on the 2-torus (q_t, p_t) phase space. If the momentum is replaced by the discrete time velocity,

$$(q_t, p_t) \to \left(x_t, \frac{x_t - x_{t-1}}{\Delta t} \right) , \tag{5}$$

and the time step set to $\Delta t = 1$, a cat map can be brought to the Percival-Vivaldi 'two-configuration representation' [76]

$$\begin{pmatrix} x_t \\ x_{t+1} \end{pmatrix} = A_{PV} \begin{pmatrix} x_{t-1} \\ x_t \end{pmatrix} - \begin{pmatrix} 0 \\ m_t \end{pmatrix} , \qquad A_{PV} = \begin{pmatrix} 0 & 1 \\ -1 & s \end{pmatrix} , \tag{6}$$

with matrix A_{PV} acting on the 2-dimensional space of successive configuration points (x_{t-1}, x_t), and integer m_t's implementing the mod 1 operation by ensuring that if x_{t-1}, x_t are within the prescribed unit interval, so is x_{t+1}.

Percival-Vivaldi cat map (6) is a discrete time non-autonomous Hamiltonian system, time-forced by pulses m_t. The integers m_t can be interpreted as 'winding numbers' [59], or, as they shepherd stray points back into the unit torus, as 'stabilising impulses' [76]. Here we shall refer to them -in field-theoretical parlance- as 'sources'. The m_t translations reshuffle the phase space, as in figure 1, thus partitioning it into regions $\mathcal{M}_m$, labeled with 'letters' m of the $|\mathcal{A}|$-letter alphabet $\mathcal{A}$, and associating a symbol sequence $\{m_t\}$ to the dynamical trajectory $\{x_t\}$. As the relation (6) between the trajectory x_t and its symbolic dynamics encoding m_t is linear, Percival and Vivaldi refer to m_t as a 'linear code'.

The deep problem with the Percival-Vivaldi code prescription is that it does not yield a generating partition; the borders (i.e., x_0, x_1 axes) of their unit-square partition $(x_{t-1}, x_t) \in (0, 1] \times (0, 1]$ do not map onto themselves, resulting in the infinity of, to us unknown, grammar rules for inadmissible symbol sequences. Percival-Vivaldi symbolic dynamics is discussed at length in the companion paper [48].

This problem was resolved in 1967 by Adler and Weiss [1, 2, 5] who utilized the stable/unstable manifolds of the fixed point at the origin to cover a unit area torus by a two-rectangles generating partition; for the Percival-Vivaldi cat map (6), such partition [31]is drawn in figure 1. Following Bowen [19], one refers to parallelograms in figure 1 as 'rectangles'. (For details see Devaney [32], Robinson [84], or ChaosBook [31]. Siemaszko and Wojtkowski [88] refer to such partitions as the 'Berg partitions', and Creagh [24] generalizes them to weakly nonlinear mappings.) Symbolic dynamics on this partition is a subshift of finite type, with the 3-letter alphabet

$$\mathcal{A} = \{\underline{1}, 0, 1\} \tag{7}$$

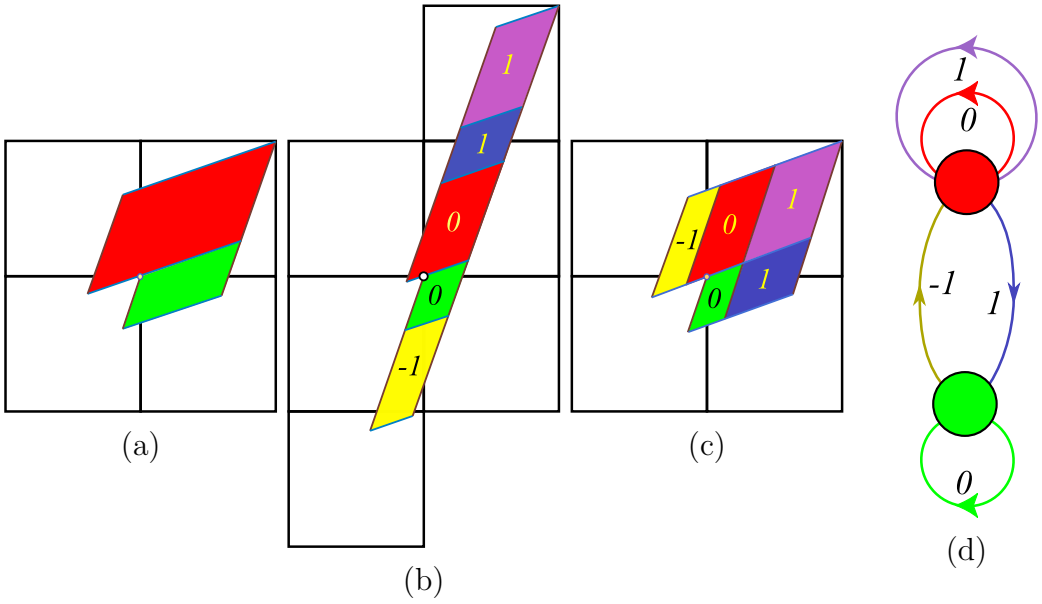

Figure 1. (Color online) (a) An Adler-Weiss generating partition of the unit torus for the $s = 3$ Percival-Vivaldi cat map (6), with rectangle $\mathcal{M}_A$ (red) and $\mathcal{M}_B$ (green) borders given by the cat map stable (blue) and unstable (dark red) manifolds, i.e., along the two eigenvectors corresponding to the eigenvalues (4). (b) Mapped one step forward in time, the rectangles are stretched along the unstable direction and shrunk along the stable direction. Sub-rectangles $\mathcal{M}_j$ that have to be translated back into the partition are indicated by color and labeled by their lattice translation $m_j \in \mathcal{A} = \{\underline{1}, 0, 1\}$, which also doubles as the 3-letter alphabet $\mathcal{A}$. (c) The sub-rectangles $\mathcal{M}_j$ translated back into the initial partition yield a generating partition, with (d) the finite grammar given by the transition graph for this partition. The nodes refer to the rectangles A and B, and the five links correspond to the five sub-rectangles induced by one step forward-time dynamics (Ffor details consult ChaosBook [31]).

that indicates the translation needed to return the given sub-rectangle $\mathcal{M}_j$ back into the two-rectangle partition $\mathcal{M} = \mathcal{M}_A \cup \mathcal{M}_B$.

While Percival and Vivaldi were well aware of Adler-Weiss partitions, they felt that their "coding is less efficient in requiring more symbols, but it has the advantage of linearity." Our construction demonstrates that one can have both: an Adler-Weiss generating cat map partition, and a linear code. The only difference from the Percival-Vivaldi formulation [76] is that one trades the single unit-square cover of the torus of (6) for the dynamically intrinsic, two-rectangles cover of figure 1, but the effect is magic - now every infinite walk on the transition graph of figure 1 (d) corresponds to a unique admissible orbit $\{x_t\}$, and the transition graph generates all admissible itineraries $\{m_t\}$.

To summarize: an explicit Adler-Weiss generating partition, such as figure 1, completely solves the Hamiltonian cat map problem, in the sense that it generates all admissible orbits. Rational and irrational initial states generate periodic and ergodic orbits, respectively [59, 77], with every phase space orbit uniquely labeled by an admissible bi-infinite itinerary of symbols from alphabet $\mathcal{A}$.

3. Life of a single Lagrangian cat

The discrete time Hamilton's equations (1,2) induce temporal evolution on a 2-torus *phase space*. For the problem at hand, it pays to go from the Hamiltonian (configuration, momentum) phase space formulation to the Lagrangian (x_{t-1}, x_t) *state space* formulation, as in (5). Indeed, written out explicitly, the Percival-Vivaldi map (6) is a 2-step difference equation of a particularly elegant form:

$$x_{t+1} - s\, x_t + x_{t-1} = -m_t\,, \tag{8}$$

with the unique integer "winding number" m_t at time step t ensuring that x_t lands in the prescribed unit interval. Here the mod 1 is enforced by integers $m_t \in \mathcal{A}$, where $\mathcal{A}$ is finite, s-dependent alphabet of possible values for m_t,

$$\mathcal{A} = \{\underline{1}, 0, \ldots s-1\}\,, \tag{9}$$

necessary to keep x_t for all times t within the unit interval $[0, 1)$ (we find it convenient to have symbol $\underline{m}$ denote m_t with the negative sign, i.e., '$\underline{1}$' stands for symbol '-1').

This 2-step difference equation can be interpreted as the second order discrete time derivative d^2/dt^2, with the time step set to $\Delta t = 1$,

$$\Box\, x_t \equiv x_{t+1} - 2x_t + x_{t-1} = (s-2)x_t - m_t\,. \tag{10}$$

But that is nothing but Newton's Second Law: "acceleration equals force." In other words, for a cat map the force $P(q) = (s-2)q$ in (2) is linear in the displacement q, so the Lagrange equations take form

$$(\Box + 2 - s)\, x_t = -m_t\,. \tag{11}$$

Depending on the value od the real parameter s, this equation is known as either the discrete Helmholtz equation (oscillatory, $s < 2$ case), or -in the case studied here- as the discrete *screened Poisson equation* (hyperbolic, damped $s > 2$ case). In Lagrangian formulation the system is no longer described by a map, only by the above equation on discrete time lattice, so instead of 'cat map' we refer to (11) as the 'temporal cat'.

The power of the linear code for the temporal cat (11) is that one can use integers m_t to encode its state space trajectories. Since the connection relation between m_t symbol sequences and x_t states is linear, it is straightforward to go back and forth between the state space points and symbolic representation of an orbit. In particular, if $\{m_t\}$ is an admissible itinerary, the corresponding field at the t time instant is given by the inverse of (11),

$$x_t = \sum_{t'=-\infty}^{\infty} g_{tt'} m_{t'}\,, \qquad g_{tt'} = \left(\frac{1}{-\Box - 2 + s}\right)_{tt'}\,, \tag{12}$$

where $g_{tt'}$ is the Green's function for one-dimensional discretized heat equation [72, 76] given explicitly, for an infinite temporal lattice, by $g_{tt'} = \Lambda^{-|t-t'|}/(\Lambda - \Lambda^{-1})$, $s = \Lambda + \Lambda^{-1}$, as defined in (4).

In the Lagrangian formulation each path is assigned an *action*, where a *path* is a set of k successive states

$$\{x_j\} = \{x_t, x_{t+1}, \cdots, x_{t+k}\}\,. \tag{13}$$

The action, whose path variation $\delta W = 0$ yields the Lagrange equations (10), can be written down by inspection:

$$W_{\{x_i\}} = \sum_{j=t}^{t+k} \left\{ \frac{1}{2}(\partial x_j)^2 + \frac{1}{2}(2-s)\, x_j^2 + m_j x_j \right\}. \tag{14}$$

Here the $[k\times k]$ matrix $\partial = (1-\sigma)/\Delta t$ is the discrete time derivative [9], and the Laplacian is given by $\Box = \partial^\top \partial = \sigma^\top \sigma - 2\mathbb{1}$, where the 1-step time shift matrix σ is non-zero on the diagonal $\sigma_{t't} = \delta_{t,t'-1}$.

[2019-08-04 Predrag] to Han - Please make sure that all definitions and signs agree with the discrete lattice sections of ChaosBook [31].

In addition, one needs to specify the boundary conditions (bc's) for the path (13). The companion article [48] deals with the Dirichlet bc's, a difficult, time-translation symmetry breaking case.

3.1. Periodic orbits

Here, however, we shall show that all that one needs to solve the temporal cat is the n-periodic, time-translation invariant choice of bc's, with periodicity of the $[n\times n]$ shift matrix σ enforced by a nonvanishing term in the lower-right corner, $\sigma_{0n} = 1$. The action (14) of state defined on an n_p-periodic path

$$\mathsf{X}_p^\top = \mathsf{X}_{m_1 m_2 \cdots m_{n_p}}^\top = (x_1, x_2, \cdots, x_{n_p})\,, \quad x_{t+n_p} = x_t\,, \tag{15}$$

is then

$$W_p = \frac{1}{2}\mathsf{X}^\top \mathsf{H}\, \mathsf{X} + \mathsf{X}^\top \mathsf{M}_p = \frac{1}{2}\sum_{t,t'=1}^{n_p} x_{t'} H_{t't} x_t + \sum_{t=1}^{n_p} m_t x_t\,, \tag{16}$$

where the symmetric $[n_p\times n_p]$ matrix $H_{tt'} = \partial^2 W_p/\partial x_t \partial x_{t'}$ of second variations of the action,

$$\mathsf{H} = s\mathbb{1} - \sigma_j - \sigma_j^\top = \begin{pmatrix} s & -1 & 0 & 0 & \dots & 0 & -1 \\ -1 & s & -1 & 0 & \dots & 0 & 0 \\ 0 & -1 & s & -1 & \dots & 0 & 0 \\ \vdots & \vdots & \vdots & \vdots & \ddots & \vdots & \vdots \\ 0 & 0 & \dots & \dots & \dots & s & -1 \\ -1 & 0 & \dots & \dots & \dots & -1 & s \end{pmatrix}, \tag{17}$$

is called the Hessian. Due to the fact that for the cat map the temporal stability multipliers (4) are the same for all orbits p of the same period n_p, this Hessian depends only on the period of orbit. That does not hold for general nonlinear cat maps [24], where each periodic orbit has its own stability.

The form of the action (14) was easy to guess, because for $0 \leq s < 2$ this is the action for a 1-dimensional chain of nearest-neighbor coupled oscillators. Here we are, however, interested in the everywhere hyperbolic, unstable case $s \geq 2$. The key property of hyperbolic flows is that nearby trajectories can *shadow* each other for finite times controlled by their stability exponents. One common way to quantify 'nearness' is to determine the minimal Euclidean distance between pairs of trajectories. That kind of distance is not invariant under symplectic transformations, and is thus meaningless in the Hamiltonian phase space. Here the notion of action comes to rescue: *the symplectic invariant distance between a pair of shadowing orbits is given by the difference of their actions* [65].

To summarize: the Lagrangian formulation requires only temporal lattice states and their actions, replacing the 'cat map' (3) by a 'temporal cat' lattice (11). The temporal cat has no generating partition analogue of the Adler-Weiss partition for a Hamiltonian cat map. As we shall now show, not only is no such partition needed to solve the system, but the Lagrangian, temporal 1-dimensional lattice formulation is the bridge that takes us from the traditional cat map (3) to the higher–dimensional coupled "multi-particle" spatiotemporal lattices (35).

4. Periodic orbits theory of cat maps

4.1. Counting Hamiltonian cat map periodic orbits

2CB

The five sub-rectangles $\mathcal{M}_j$ of the two-rectangle Adler-Weiss partition of figure 1 (c) motivate introduction of a 5-letter alphabet

$$\bar{\mathcal{A}} = \{1,2,3,4,5\} = \{A^0A, B^1A, A^1A, B^0B, A^{\bar{1}}B\}\,, \tag{18}$$

see figure 2 (b), which encodes the links of the transition graph of figure 1 (d). The loop expansion of the determinant [26] of the transition graph T of figure 2 (b) is given by all non-intersecting walks on the graph

$$\det(1-zT) = 1 - z(t_1+t_3+t_4) - z^2(t_{25} - (t_1+t_3)t_4)\,, \tag{19}$$

where t_p are traces over fundamental cycles, the three fixed points $t_1 = T_{A^0A}, t_3 = T_{A^1A}, t_4 = T_{B^0B}$, and the 2-cycle $t_{25} = T_{B^1A}T_{A^{\bar{1}}B}$.

As the simplest application, consider counting all admissible cat map periodic orbits. This is accomplished by setting the non-vanishing links of the transition graph to $T_{ji} = 1$, resulting in the cat map topological zeta function [31, 52],

$$1/\zeta_{\rm top}(z) = \frac{1-3z+z^2}{(1-z)^2}\,, \tag{20}$$

where the numerator $(1-z)^2$ corrects the overcounting of the fixed point at the origin due to assigning it to both $\mathcal{M}_A$ (twice) and $\mathcal{M}_B$ rectangles [70] (see figure 3 (a) for an example of such over-counting). As explained in ChaosBook [26], the topological zeta

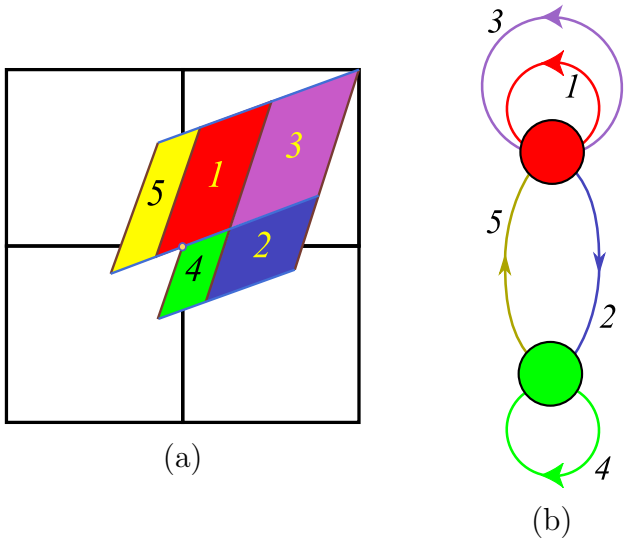

Figure 2. (Color online) (a) The sub-rectangles $\mathcal{M}_j$ of figure 1 (c). (b) Admissible orbits correspond to walks on the transition graph of figure 1 (d), with rectangles $\mathcal{M}_A$ (red) and $\mathcal{M}_B$ (green) as nodes, and the links labeled by 5-letter alphabet (18), see the loop expansion (19).

function (20) counts the numbers of prime cycles. For the $s = 3$ cat map example at hand, they are

$$\{M_j\} = (M_1, M_2, M_3, M_4, M_5, \cdots) = (1, 2, 5, 10, 24, \cdots)\,, \tag{21}$$

in agreement with the Bird and Vivaldi [14] census.

This derivation was based on the Adler-Weiss generating partition, a clever explicit visualization of the cat map dynamics, whose generalization to several coupled maps (let alone spatially infinite coupled cat maps lattice) is far from obvious: one would have to construct covers of high-dimensional parallelepipeds by sets of sub-volumes. However, as Keating [59] explains, no such explicit generating partition is needed to count cat map periodic orbits. Cat map (6) periodic points are the fixed points of

$$\begin{bmatrix} q_t \\ p_t \end{bmatrix} = \begin{bmatrix} q_{t+n} \\ p_{t+n} \end{bmatrix} = A^n \begin{bmatrix} q_t \\ p_t \end{bmatrix} \mod 1\,,$$

so on the unwrapped phase space lattice, tiled by repeats of the unit square of the cat map torus,

$$(A^n - \mathbf{1}) \begin{bmatrix} q_t \\ p_t \end{bmatrix} = \begin{bmatrix} m_t^q \\ m_t^p \end{bmatrix}\,, \qquad (m_t^q, m_t^p) \in \mathbb{Z}^2\,, \tag{22}$$

matrix $(A^n - \mathbf{1})$ stretches the unit square into what Keating calls the 'fundamental parallelogram' (an example is drawn in figure 3). The number of periodic points of period n is given by the area of this parallelogram

$$N_n = |\det(A^n - \mathbf{1})| = \Lambda^n + \Lambda^{-n} - 2\,, \tag{23}$$

where the Λ is the stability multiplier (4) of the Hamiltonian time evolution matrix A in (3). Ozorio de Almeida and Hannay [4] were the first to state (23) as an illustration of their 'principle of uniformity': periodic points of an ergodic system, counted with their natural weighting, are uniformly dense in phase space.

Substituting the numbers of periodic points N_n into the *topological* or *Artin-Mazur* zeta function [6, 26] we obtain

$$\begin{aligned} 1/\zeta_{\rm top}(z) &= \exp\left(-\sum_{n=1}^{\infty}\frac{z^n}{n}N_n\right) = \exp\left(-\sum_{n=1}^{\infty}\frac{z^n}{n}(\Lambda^n+\Lambda^{-n}-2)\right) \\ &= \exp\left[\ln(1-z\Lambda)+\ln(1-z\Lambda^{-1})-2\ln(1-z)\right] \\ &= \frac{(1-z\Lambda)(1-z\Lambda^{-1})}{(1-z)^2} \\ &= \frac{1-sz+z^2}{(1-z)^2}\,, \end{aligned} \tag{24}$$

in agreement with Isola [52], as well as the Adler-Weiss generating partition topological zeta function (20). As explained in ChaosBook [26], topological zeta functions count *prime* orbits (21), i.e., the time invariant sets of periodic points, rather that the individual periodic points.

4.2. Counting Lagrangian temporal cat periodic orbits

We now rederive the number of periodic points (23) using the Lagrangian formulation. This is essential to all that follows, as the Lagrangian formulation will apply to spatiotemporal cat in any dimension.

For Hamiltonian evolution (3) the linear stability [2×2] matrix Jacobian matrix A^n describes the growth of an initial state perturbation in n steps. For Lagrangian system (16), the first variation of the action $\delta W = 0$ yields the Lagrangian equations of motion (11), while the second variation, the $[n\times n]$ Hessian matrix (17), describes the stability the *entire* given periodic orbit.

[2019-08-08 Predrag] Introduce Toeplitz, discrete Fourier, Chebyshev

For Lagrangian systems the number of periodic points $\{x_t\}$ is given by the determinant of the Hessian matrix (17). All admissible solutions of period n are constrained to a unit volume n-dimensional hypercube, with all the state values within $0 \le x_t < 1$. This hypercube is stretched to an n-dimensional parallelepiped by the Hessian matrix (17), with each of the integer points inclosed within the stretched parallelepiped corresponding to a periodic solution of period n. Now the number of periodic orbits is the number of integer points enclosed in a parallelepiped, given by its volume $\det H$. As the Hessian (17) is a Toeplitz matrix (a matrix that is constant along each diagonal, i.e., $H_{jk} = h_{j-k}$), we can diagonalize it by a discrete Fourier transform, so this volume is given by the product of eigenvalues of H,

$$N_n = \det H = \prod_{j=0}^{n-1}\left[s - 2\cos\left(\frac{2\pi j}{n}\right)\right]\,. \tag{25}$$

Using the standard theory of Toeplitz matrices (basically the orthonormality of discrete Fourier eigenmodes), one can write this determinant compactly as

$$N_n = \det H = 2\,T_n(s/2) - 2\,, \tag{26}$$

where $T_n(s/2)$ is the Chebyshev polynomial of the first kind.

[2018-12-01 Predrag] Give references!

[2017-09-20 Predrag] Probably should do circulants first, in the spirit of starting out with the infinite lattice case (12).

[2018-12-01 Han] I still have to derive and recheck this formula!

4.3. Hill's formula

[2018-12-01 Predrag] What Hill's formula? Is it (D.6)?
discrete Hill's formula [17]:

$$\det(A^n - \mathbf{1}) = \frac{(-1)^n \det H}{\prod_{i=1}^{n} \det B_i}\,, \tag{27}$$

where for the one dimensional cat map the B here is an $[1\times 1]$ matrix:

$$B = -\frac{\partial^2 L(x_{n+1}, x_n)}{\partial x_{n+1} \partial x_n} = 1\,, \tag{28}$$

According by the discrete Hill's formula [17, 68] these two expressions are equivalent:

$$|\det(A^n - \mathbf{1})| = \det H\,. \tag{29}$$

To summarize: as the cat map hyperbolicity is the same everywhere and does not depend on a particular solution X_p, counting periodic orbits is all that is needed to solve a cat-map dynamical system completely; once periodic orbits are counted, all cycle averaging formulas [25] follow.

4.4. An example: fundamental parallelogram for 2-cycles

To visualize the fundamental parallelogram (22) counting of periodic solutions, consider Percival-Vivaldi $s = 3$ cat map (6) acting on states x_t within the unit square $(x_{t-1}, x_t) \in (0, 1] \times (0, 1]$, as in figure 3 (a). In 2 time steps matrix $(A^2 - \mathbf{1})$ stretches the unit square into the fundamental parallelogram, with integer points within the parallelogram corresponding to periodic points of period 2. Note however that the integer points on the vertices of the fundamental parallelogram over-count the number distinct solutions, as was already noted in the construction of the topological zeta function (20).

This overcounting is an artifact of the choice of the initial unit square. If initial states lie within the symmetric unit square $(-1/2, 1/2] \times (-1/2, 1/2]$, the fundamental parallelogram figure 3 (b) all 5 integer points lie within the fundamental parallelogram, without any over-counting. The $(x_{t-1}, x_t) = (0, 0)$ solution is a repeat of the fixed point solution for $n = 1$, so the total number of period-2 prime cycles is 2, as given in (21).

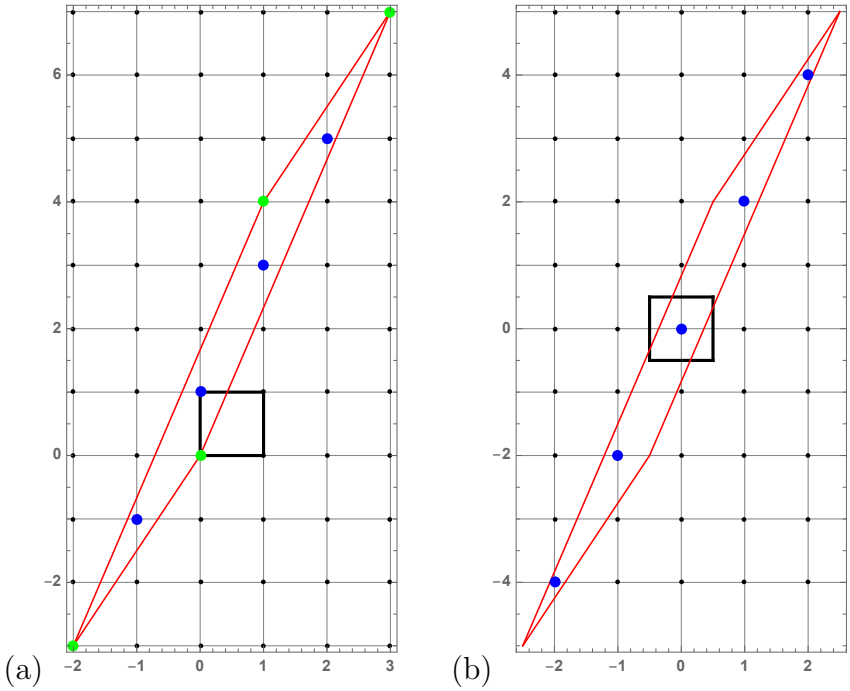

Figure 3. (Color online) (a) The corner-centered [black] unit square $(0,1] \times (0,1]$ is stretched by $(A^2 - \mathbf{1})$ into the [red] fundamental parallelogram. By (22), each integer point within the fundamental parallelogram corresponds to a periodic point solution of period 2. The 4 internal integer points are marked by the blue dots. Note however that the 4 vertex integer points [green] are the same point mod 1, and thus have to be counted as 1 fixed point solution. (b) The face-centered [black] unit square $(-1/2, 1/2] \times (-1/2, 1/2]$ is stretched by $(A^2 - \mathbf{1})$ into the [red] fundamental parallelogram. Now all 5 integer points [blue] are within the fundamental parallelogram, yielding again 5 periodic point solutions of period 2, but without any over-counting. Percival-Vivaldi cat map (6), $s = 3$.

4.5. An example: Hessian for 2- and 3-cycles

The Hessians of temporal cats solutions are much harder to visualize, as a period-2 solution temporal cat is a 2-torus, period-3 solution a 3-torus, etc., see figure 4. For for $n > 3$ temporal cat and 2- and d-dimensional spatiotemporal cat there are no useful visualizations of corresponding Hessians.

4.6. An example: 4-cycles

As a hands-on example, let us count the $M_4 = 10$ admissible prime 4-cycles, as stated in (21). The admissible blocks M_p can be read off as walks on either the 5-letter alphabet (18) graph, see figure 2 (b), or the 3-letter alphabet (7) graph, see figure 1 (d). They are, in 5-letter (top), and 3-letter (bottom) alphabets

$\overline{1113}$	$\overline{1125}$	$\overline{1245}$	$\overline{1253}$	$\overline{1325}$
0001	0011	0101	0111	0111

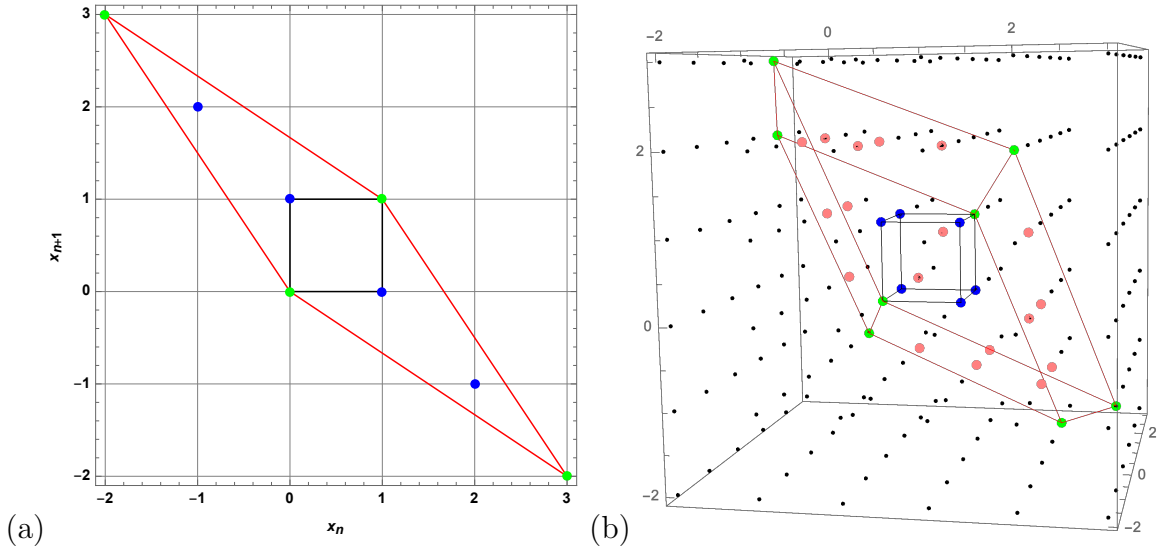

Figure 4. (a) A 2-dimensional corner-centered [black] unit square stretched by the 2-cycle Hessian H_2. The blue dots are internal integer points in the [red] stretched parallelogram. The four green dots on the vertices of the parallelogram are counted as the one fixed point. (b) A 3-dimensional corner-centered [black] unit-cube stretched by H_3. The blue dots are internal integer points in the [red] stretched parallelepiped. The green dots are on the vertices of the parallelepiped. The pink dots are on the surface of the parallelepiped.

$$\begin{array}{ccccc} \overline{1133} & \overline{3325} & \overline{3331} & \overline{3245} & \overline{4452} \\ 0011 & 111\underline{1} & 1110 & 110\underline{1} & 00\underline{11} \end{array} \quad . \tag{30}$$

The corresponding periodic orbits X_p are computed using Green's function (12) (the inverse of the $[4 \times 4]$ Hessian (17), easiest to evaluate by discrete Fourier transforms):

$$\mathsf{M}_{0001} \Rightarrow \quad \mathsf{X}_{0001} = g \begin{bmatrix} 0 \\ 0 \\ 0 \\ 1 \end{bmatrix} = \frac{1}{15} \begin{bmatrix} 3 \\ 2 \\ 3 \\ 7 \end{bmatrix} \quad .$$

Likewise,

$$\begin{aligned} \mathsf{X}^\top_{001\underline{1}} &= \frac{1}{15} \begin{bmatrix} -1 & 1 & 4 & -4 \end{bmatrix} , & \mathsf{X}^\top_{010\underline{1}} &= \frac{1}{15} \begin{bmatrix} 0 & 5 & 0 & -5 \end{bmatrix} \\ \mathsf{X}^\top_{01\underline{1}1} &= \frac{1}{15} \begin{bmatrix} 4 & 6 & -1 & 6 \end{bmatrix} , & \mathsf{X}^\top_{011\underline{1}} &= \frac{1}{15} \begin{bmatrix} 2 & 8 & 7 & -2 \end{bmatrix} \\ \mathsf{X}^\top_{0011} &= \frac{1}{15} \begin{bmatrix} 5 & 5 & 10 & 10 \end{bmatrix} , & \mathsf{X}^\top_{111\underline{1}} &= \frac{1}{15} \begin{bmatrix} 9 & 11 & 9 & 1 \end{bmatrix} \\ \mathsf{X}^\top_{1110} &= \frac{1}{15} \begin{bmatrix} 12 & 13 & 12 & 8 \end{bmatrix} , & \mathsf{X}^\top_{110\underline{1}} &= \frac{1}{15} \begin{bmatrix} 7 & 8 & 2 & -2 \end{bmatrix} \\ \mathsf{X}^\top_{00\underline{11}} &= \frac{1}{15} \begin{bmatrix} 1 & -1 & -4 & 4 \end{bmatrix} . \end{aligned} \tag{31}$$

One can verify that for each of these prime 4-cycles all periodic points (x_t, x_{t+1}) are within the rectangles $\mathcal{M}_A$ or $\mathcal{M}_B$ of figure 1 (b), in the temporal order dictated by the transition graph, and thus all admissible.

5. Spatiotemporal cat

[2016-11-08 Predrag] Be careful: This section might in parts have text snippets identical to the ones used in GHJSC16.tex [48]. Eliminate duplications!

We now turn to generalizing the 1-dimensional temporal cat to the d-dimensionalspatiotemporal cat, with cat maps on sites ("particles") coupled to their nearest neighbors on a spatiotemporally infinite $\mathbb{Z}^d$ lattice. To motivate this 'turbulent' field theory, we briefly review the early work on coupled map lattices (CMLs), and then describe the new results specific to our system of L^d, $L \to \infty$ coupled "particles." The spatiotemporal cat is introduced in section 5.2, and solved in section 6.

5.1. Coupled map lattices

In order to solve a partial differential equation (PDE) on a computer, one has to represent it by a finite number of computational elements. The simplest discretization of a scalar spacetime field $x(q,\tau)$ is by specifying its values $x_{nt} = x(q_n, \tau_t)$ on lattice points $(n,t) \in \mathbb{Z}^2$. Once spatial and temporal derivatives are replaced by their discretizations, the PDE evolution has been reduced to dynamics of a coupled map lattice, a spatially extended system with discrete time, discrete space, and continuous state (field) variables. For the problem a hand, CML conceptual advantage is not only numerical, but also that the technical problems such as existence and uniqueness of PDEs are regularized away, and the essence of spatiotemporal chaos is revealed in a transparent form.

In a Euclidean field theory one couples the neighbors harmonically, and thinks of this starting, free field theory formulation as a spring mattress [92] to which weakly coupled nonlinear terms are then added. Similarly, the conventional CML models, mostly motivated by discretizations of dissipative PDEs, start out with chaotic on-site dynamics weakly coupled to neighboring sites, with strong space-time asymmetry. An example are diffusive coupled map lattices, introduced by Kaneko [55, 56], with time evolution given by

$$\begin{aligned} x_{n,t+1} &= g(x_{nt}) + \epsilon[g(x_{n-1,t}) - 2g(x_{nt}) + g(x_{n+1,t})] \\ &= (1 + \epsilon\,\Box)g(x_{nt})\,, \end{aligned} \tag{32}$$

where the individual spatial site's dynamical system $g(x)$ is a 1-dimensional map, such as the logistic map, coupled diffusively to its nearest neighbors by $\Box$, the Laplacian for the discretized second order *spatial* derivative d^2/dx^2, with the lattice spacing constant set equal to unity.

The form of time-step map $g(x_{nt})$ is the same for all times, i.e., the law of temporal evolution is invariant under the group of discrete *time translations*. Spatially homogenous lattice models also invariant under discrete *space translations* were studied by Bunimovich and Sinai [20] in the case when $g(x_{nt})$ is a one-dimensional expanding map. For quantum mechanics and statistical mechanics applications, one needs the dynamics to be Hamiltonian, motivating models such as coupled standard map

lattice [57] and ϕ^4 lattice [51]. Pesin and Sinai [78] were the first to study such lattices, with chains of coupled Anosov maps. In order to establishe rigorously the desired statistical properties of coupled map lattices, such as the continuity of their SRB measures, they, and most of the subsequent statistical mechanics literature, relied on the structural stability of Anosov automorphisms under small perturbations. For such lattices the neighboring sites have to be coupled sufficiently weakly (small ϵ in (32)) so that the site cat maps could be conjugated to a lattice of uncoupled Anosov automorphisms, with a finite Markov partition, the key ingredient required for the proofs.

Contrast this with the Gutkin-Osipov [47] *spatiotemporal cat*

$$(-\Box + s - 4)\, x_z = m_z \tag{33}$$

to be studied here. The equation is space $\leftrightarrow$ time symmetric and has the temporal and spatial dynamics coupled as strongly as possible, with $\epsilon \approx O(1)$ in (32). Unlike the systems studied in [20], spatiotemporal cat cannot be conjugated to a product of non-interacting cat maps. Spatiotemporal cat is arguably the simplest example of a classical field theory for which the local degrees of freedom are hyperbolic rather than oscillatory ("inverted pendula"). As we shall now show, it is also a field theory for which all admissible spatiotemporal patterns can be enumerated, and identify their recurrences (shadowing of a large invariant 2-torus by smaller invariant 2-tori) identified.

5.2. d-dimensional spatiotemporal cat

Now that we have mastered the *temporal cat* (11), a generalization to the *spatiotemporal cat* (33) is immediate. Consider a 1-dimensional spatial lattice, with field x_{nt} (the angle of a kicked rotor "particle" at instant t) at spatiotemporal site (n, t). If each site couples only to its nearest neighbors $x_{n\pm1,t}$, and if we require (1) invariance under spatial translations, (2) invariance under spatial reflections, and (3) invariance under the space-time exchange, we arrive at the 2-dimensional Euclidean lattice difference equations:

$$x_{n,t+1} + x_{n,t-1} - s\, x_{nt} + x_{n+1,t} + x_{n-1,t} = -m_{nt}\,. \tag{34}$$

More generally, the same argument yields the screened Poisson equation (11) for the d-dimensional *spatiotemporal cat*

$$\begin{aligned}(\Box + 2d - s)\, x_z = \; - m_z\,, \qquad x_z \in \mathbb{T}^1\,, \quad m_z \in \mathcal{A}\,, \quad z \in \mathbb{Z}^d\,,\\ \mathcal{A} = \{-2d+1, -2d+2, \cdots, s-2, s-1\}\,,\end{aligned} \tag{35}$$

where $\Box$ is the discrete d-dimensional Euclidean space-time Laplacian. The key insight (an insight that applies to coupled-map lattices [79, 80, 82], and PDEs modeled by them, not only the system considered here) is that a d-dimensional spatiotemporal field $\{x_z\} = \{x_z, z \in \mathbb{Z}^d\}$ has to be described by a corresponding *d-dimensional* spatiotemporal symbol block $\{m_z\} = \{m_z, z \in \mathbb{Z}^d\}$, rather than a 1-dimensional temporal symbol sequence, as one does when describing a finite coupled "N-particle" system in the Hamiltonian formalism.

Starting with the theory of $d = 1$ temporal cat developed in section 3, it will suffice to work out the $d = 2$ spatiotemporal cat in some detail to understand the general case.

5.3. 2-dimensional spatiotemporal cat

While the $d = 2$ spatiotemporal cat does have a Hamiltonian formulation [47], its Lagrangian formulation as screened Poisson equation (33), in analogy with the temporal cat (11), is a natural departure point for what follows:

$$(-\Box + s - 4)\, x_{nt} = m_{nt}\,, \qquad x_{nt} \in \mathbb{T}^1\,, \quad m_{nt} \in \mathcal{A}\,, \quad (n,t) \in \mathbb{Z}^2\,,$$
$$\mathcal{A} = \{\underline{3}, \underline{2}, \underline{1}, 0, \cdots, s-2, s-1\}\,, \tag{36}$$

where $\Box$ is now the discrete 2-dimensional space-time Laplacian on $\mathbb{Z}^2$,

$$\Box\, x_{nt} = x_{n,t-1} + x_{n-1,t} - 4\, x_{nt} + x_{n,t+1} + x_{n+1,t}\,. \tag{37}$$

Gutkin and Osipov [47] refer to equation (36) as the 'non-perturbed coupled cat map'. Sources $m_{nt} \in \mathcal{A}$ are necessary to keep the 'rotor state' x_{nt} on every site within a unit interval. The symbol $\underline{m_t}$ here denotes m_t with the negative sign, i.e., '$\underline{3}$' stands for symbol '-3'. As we now show, the block $\mathsf{M} = \{m_{nt} \in \mathcal{A},\ (n,t) \in \mathbb{Z}^2\}$ can be used as a 2-dimensional symbolic representation of the lattice system state. By the linearity of equation (36), every solution X can be uniquely recovered from its symbolic representation M. Inverting (36) we obtain

$$x_z = \sum_{z' \in \mathbb{Z}^2} g_{zz'} m_{z'}, \qquad g_{zz'} = \left(\frac{1}{-\Box + s - 4} \right)_{zz'}\,, \tag{38}$$

where $g_{zz'}$ is the Green's function for the 2-dimensional discretized screened Poisson equation. However, a given lattice block M is *admissible* if and only if all $x_z \in \mathsf{X}$ given by (38) fall into the interval $[0, 1)$.

A key advantage of the spatiotemporal code M is illustrated already by the $d = 2$ case. While the size of an Adler-Weiss, Hamiltonian evolution alphabet based on Markov partitions grows exponentially with the "particle number" L, the number of letters (35) of the spatiotemporal code $\mathcal{A}$ is finite and the same for any spatial extent L, including the $L \to \infty$ spatiotemporal cat. For the spatiotemporal code, a field X over a periodic spatiotemporal domain is encoded by a doubly periodic 2-dimensional block M of symbols from a small alphabet, rather then by a 1-dimensional temporal string of symbols from the exponentially large (in L) 'L-particle' alphabet $\bar{\mathcal{A}}$.

But the main advantage of the spatiotemporal cat is that it is a field theory defined on a lattice, a theory that can be solved by the well-developed crystallographic methods: in what follows, we use the notation of Dresselhaus *et al* [34]. Besides the invariance under shifts in time and space directions, spatiotemporal cat equations (36) are invariant under the space and time reflections $n \to -n$, $t \to -t$, as well as under exchange $n \longleftrightarrow t$ of space and time. Spatiotemporal cat thus has the point-group symmetries of the square lattice: rotations by $\pi/2$, and reflection across x-axis, y-axis, and diagonals a and b,

$$C_{4v} = \mathrm{D}_4 = \{E, C_{4z}^+, C_{4z}^-, C_{2z}, \sigma_y, \sigma_x, \sigma_a, \sigma_b, \}\,. \tag{39}$$

In the international crystallographic notation [34], the space group of symmetries of this square lattice is referred to as $p4mm$.

[2016-11-08 Predrag] In addition, if $\mathsf{M} = \{m_{nt}\}$ is an admissible state, so is its conjugation symmetry partner $\bar{\mathsf{M}} = \{\bar{m}_{nt}\}$, where $\bar{m}_{nt} = s - 4 - m_{nt}$.

While the spatiotemporal cat equations are invariant under the point group (39), the individual spatiotemporal cat solutions X can be invariant under subgroups of space group $p4mm$. In what follows we shall use the standard crystallographic methods to describe spatiotemporal cat in its first Brillouin zone by quotienting only its translational symmetries, and postpone the full space group reduction to a later publication.

6. Invariant tori of d-dimensional spatiotemporal cat

[2017-09-16 Predrag] Methods described above make it an easy task to obtain a particular class of invariant 2-tori for the spatiotemporal cat.
Invariant 2-torus's coordinate representation $\Gamma = \{x_z, z \in \mathbb{Z}^2_{\rm LT}\}$, is obtained by taking inverse of (36):

$$x_z = \sum_{z' \in \mathbb{Z}^2_{\rm LT}} \mathsf{g}^0_{zz'} m_{z'}, \qquad m_{z'} \in \mathcal{A}_0, \tag{40}$$

where $\mathsf{g}^0_{zz'}$ is the corresponding Green's function with periodic bc's.

We now show how to count the number of invariant tori of a d-dimensional spatiotemporal cat, and, as an example, in section 6.1 apply the method to counting invariant 2-tori of the 2-dimensional spatiotemporal cat.

The d-dimensional spatiotemporal cat satisfies screened Poisson equation (35)

$$(-\Box + s - 2d)\, x_z = m_z\,, \qquad z \in \mathbb{Z}^d\,, \tag{41}$$

where $\Box$ is the discrete d-dimensional Laplacian (discrete Laplacians on 1-dimensional and 2-dimensional lattices are given in (10) and (37)). As in (14), a d-dimensional discrete Laplacian can be written as

$$\Box = \sum_{i=1}^{d} (\sigma_i + \sigma_i^\top - 21)\,, \tag{42}$$

where σ_i is a translation (lattice shift) operator which translates the field in the positive ith direction by one lattice spacing, and its inverse $\sigma_i^\top$ translates the field in the negative ith direction. Thus the spatiotemporal cat equation (41) can be written as

$$(Hx)_z = \sum_{z'} \sum_{i=1}^{d} \left(\frac{s}{d}1 - \sigma_i - \sigma_i^\top\right)_{zz'} x_{z'} = m_z\,, \qquad z \in \mathbb{Z}^d\,. \tag{43}$$

The x_z and m_z are lattice arrays with d indices, and the Hessian $\sum(s/d - \sigma_i - \sigma_i^\top)$ (tensor) matrix (17) is a rank $2d$ tensor.

The periodicity of a periodic state $\mathsf{X}(z)$ over a d-dimensional lattice, with the state described by repeats of a Bravais primitive cell spanned by basis vectors $(\mathbf{a}_1, \mathbf{a}_2, \cdots, \mathbf{a}_d)$,

$$\mathcal{L} = \left\{ \sum_{i=1}^{d} n_i \mathbf{a}_i \;\middle|\; n_i \in \mathbb{Z} \right\}. \tag{44}$$

[2019-09-11 Predrag] copy to here the nomenclature used in *PHYS-7143-19 week8*.

A field $\mathsf{X}(z)$ is Bravais lattice periodic if it satisfies

$$\mathsf{X}(z+R) = \mathsf{X}(z)\,, \quad R \in \mathcal{L}\,. \tag{45}$$

In order to count the periodic points as we did for the temporal cat (25), we need to compute the eigenvalues and eigenvectors of the Hessian matrix (43). The eigenvalues determine the determinant of the Hessian matrix, and thus count the number of invariant d-tori. The eigenvectors enable us to diagonalize the Hessian matrix, and compute its inverse, the Green's function.

In (43) the operators, fields and sources are defined on the spatiotemporally infinite d-dimensional lattice. The spatiotemporal cat equation (43) is also satisfied on a single periodic tile, i.e. invariant d-torus, provided the translation operators satisfy the periodic bc's on the tile. Thus, in order to count the invariant d-tori, it thus suffices to determine the eigenvalues of the Hessian matrix on finite tiles.

The Hessian matrix (43) is constructed from d commuting translation operators σ_i. The eigenvectors of translation operators are plane waves

$$f_k(z) = e^{ik\cdot z}\,, \tag{46}$$

where k is a d-dimensional wave vector. A plane wave does not satisfy the periodic conditions (45), unless

$$f_k(z+R) = e^{ik\cdot z}e^{ik\cdot R} = e^{ik\cdot z}\,. \tag{47}$$

So $k\cdot R$ must equal to an integer times 2π. Since R is a site on the Bravais lattice, the wave vector k must lie in the reciprocal lattice

$$k \in \overline{\mathcal{L}}\,, \quad \overline{\mathcal{L}} = \left\{ \sum_{i=1}^{d} n_i \mathbf{b}_i \,|\, n_i \in \mathbb{Z} \right\}\,, \tag{48}$$

where basis vectors $\mathbf{b}_i$ satisfy:

$$\mathbf{b}_i \cdot \mathbf{a}_j = 2\pi\delta_{ij}\,. \tag{49}$$

To get the corresponding eigenvalue and periodic eigenvector (47), note that

$$(\sigma_j + \sigma_j^{\top})e^{ik\cdot z} = e^{i(k\cdot z - k_j)} + e^{i(k\cdot z + k_j)} = 2\cos k_j e^{ik\cdot z} = (2\cos k_j)e^{ik\cdot z}\,, \tag{50}$$

where the $k = (k_1, k_2, \cdots, k_d)$. Hence the eigenvalue of the Hessian (43) corresponding to the eigenvector (47) is

$$\lambda_k = s - 2\sum_{j=1}^{d} \cos k_j\,. \tag{51}$$

6.1. Counting invariant 2-tori

Now let us specialize to the 2-dimensional spatiotemporal cat. Gutkin and Osipov [47] refer to an screened Poisson equation invariant 2-torus solution p as a 'many-particle periodic orbit', with x_{nt} 'doubly-periodic', or 'closed,'

$$x_{nt} = x_{n+L_p,t+T_p}\,, \quad n = 0, 1, 2, \cdots, L_p - 1\,; \quad t = 0, 1, 2, \cdots, T_p - 1\,.$$

A cover of an invariant 2-torus on a 2-dimensional spatiotemporally infinite $\mathbb{Z}^2$ lattice can have a more complicated shape than a 1-dimensional temporal cat periodic orbit symbol block. An invariant 2-torus can tile the 2-dimensional square lattice not only by its repeats in the time or the space direction, but also by translations in both, with the periodicity of the tile described by a 2-dimensional Bravais lattice (44):

$$\mathcal{L} = \{n_1\mathbf{a}_1 + n_2\mathbf{a}_2 \,|\, n_i \in \mathbb{Z}\}\,. \tag{52}$$

The reciprocal lattice of the Bravais lattice (52) is spanned by reciprocal basis (49)

$$\overline{\mathcal{L}} = \{n_1\mathbf{b}_1 + n_2\mathbf{b}_2 \,|\, n_i \in \mathbb{Z}\}\,. \tag{53}$$

The eigenvectors of the translation operator have the form of a plane wave

$$f_k(z) = e^{ik\cdot z}\,, \quad k \in \overline{\mathcal{L}}\,, \tag{54}$$

and, in addition, satisfy the Bravais lattice (52) periodicity. The general form of the basis vectors of Bravais lattice (52) is $\mathbf{a}_1 = \{l_1, l_2\}$, $\mathbf{a}_2 = \{l_3, l_4\}$. The choice of the basis for a given Bravais lattice is not unique. As shown by Lind [67], one can choose basis vectors of form $\mathbf{a}_1 = \{l_1, 0\}$ and $\mathbf{a}_2 = \{l_3, l_4\}$ without loss of generality. Write the basis vectors in a matrix form:

$$\begin{bmatrix} \mathbf{a}_1 & \mathbf{a}_2 \end{bmatrix} = \begin{bmatrix} l_1 & l_3 \\ 0 & l_4 \end{bmatrix}\,. \tag{55}$$

Then the basis vectors of the reciprocal lattice are:

$$\begin{bmatrix} \mathbf{b}_1 & \mathbf{b}_2 \end{bmatrix} = \frac{2\pi}{l_1 l_4}\begin{bmatrix} l_4 & 0 \\ -l_3 & l_1 \end{bmatrix}\,. \tag{56}$$

The Bravais lattice and reciprocal lattice are shown in figure 5. A plane wave with wave vector k in the reciprocal lattice $\overline{\mathcal{L}}$ is an eigenvector of the Hessian matrix (43) that satisfies the periodic condition of Bravais lattice $\mathcal{L}$. The eigenvector with wave vector $k = n_1\mathbf{b}_1 + n_2\mathbf{b}_2$ is

$$f_k(z) = e^{ik\cdot z} = \exp\left(i\frac{2\pi}{l_1 l_4}(n_1 l_4 z_1 - n_1 l_3 z_2 + n_2 l_1 z_2)\right)\,, \tag{57}$$

where the $z = (z_1, z_2)$, with the Hessian matrix eigenvalue

$$\lambda_k = \sum_{j=1}^{2}\frac{s}{2} - 2\cos k_j = s - 2\cos 2\pi(\frac{n_1}{l_1}) - 2\cos 2\pi(\frac{n_1 l_3}{l_1 l_4} - \frac{n_2}{l_4})\,. \tag{58}$$

As the field has support only on the square lattice sites, it suffices to use the wave vectors $k = n_1\mathbf{b}_1 + n_2\mathbf{b}_2$ with n_1 from 0 to $l_1 - 1$ and n_2 from 0 to $l_4 - 1$ to get all of

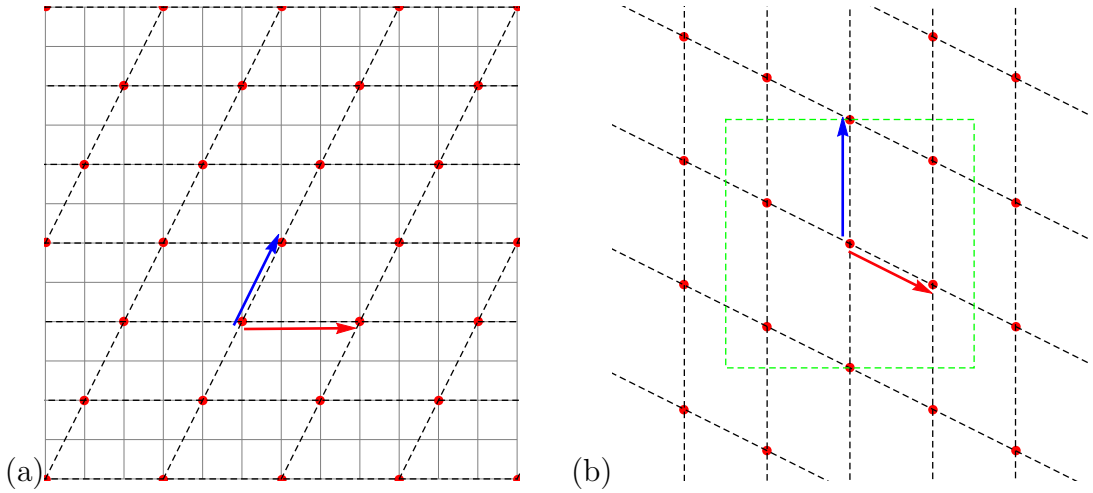

Figure 5. (Color online) (a) The intersections of the (light grey) solid lines form the square lattice on which the discrete field x_z is defined. The (red) vector $\mathbf{a}_1 = (3, 0)$ and the (blue) vector $\mathbf{a}_2 = (1, 2)$ are our example of an Bravais lattice basis vectors pair. The intersections (red points) of the black dashed lines form the Bravais lattice $\mathcal{L}$, i.e., the tiles (invariant 2-tori) on which the field is periodic. (b) The reciprocal lattice (49). Each reciprocal lattice point is a wave vector of the eigenvector of the translation operator with periodicity given by the Bravais lattice. The green dashed square encloses the first Brillouin zone of the *square lattice* (not the Bravais lattice). The wave vectors in the first Brillouin zone give all eigenvectors of the translation operator. Any wave vector outside of the first Brillouin zone is equivalent to a wave vector within it.

the reciprocal lattice eigenvectors. This range contains all of the wave vectors in one lattice cell of reciprocal lattice of the square lattice, as shown in figure 6, where wave vectors with n_1 from 0 to $l_1 - 1$, and n_2 from 0 to $l_4 - 1$ are enclosed by the green dashed square. Any wave vector on the reciprocal lattice $\overline{\mathcal{L}}$ outside of this range will give an eigenvector which is equivalent to an eigenvector with the wave vector within this range. So the number of eigenvectors is $l_1 l_4$, which is the number of square lattice sites within the minimal repeating tile. Given a Bravais lattice, the choice of the lattice cell is not unique, but the area of the lattice cell is given by the wedge product of the two basis vectors, which is also the number of the square lattice sites in this lattice cell.

[2019-06-25 Han] Is the lattice cell called the primitive cell?
[2019-08-06 PC] I do not think "lattice cell" is the standard terminology, and as you have chosen not to quotient the point group, what you have is not 'primitive' - that would be 1/8th triangle that tiles the first Brillouin zone, I think. Please strictly follow the nomenclature of a single reference -presumably Dresselhaus *et al* [34] in your case- and state so clearly in your text. Whenever you use a reference, ethics of the profession requires that you clearly cite it.

Given the eigenmodes with a given periodic condition, one can reduce the 2-dimensional square lattice to a finite repeating tile. The screened Poisson equation in this tile is still (43). But now the field and source are define in a $[l_1 \times l_4]$ lattice. And

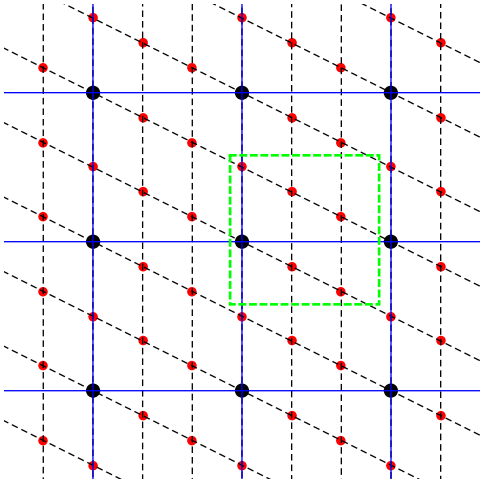

Figure 6. (Color online) The reciprocal lattices of both the Bravais lattice $\mathcal{L}$ and the square lattice. The red points are the reciprocal lattice of the Bravais lattice in figure 5 (a). The black points are the reciprocal lattice of the square lattice. Each of these squares enclosed by the blue lines has edge length 2π. And these squares are also repeating unit of the wave vectors (the red dots in this figure). Two wave vectors are equivalent if they are different by a vector on the reciprocal lattice of the square lattice.

the Hessian (43) is a rank 4 tensor with indices in a finite range. The Hessian has $l_1 l_4$ eigenmodes. We know that the number of invariant 2-tori is equal to the determinant of the Hessian, which is the product of all the eigenvalues:

$$N = \prod_k \lambda_k = \prod_{n_1=0}^{l_1-1} \prod_{n_2=0}^{l_4-1} \left[s - 2\cos(\frac{2\pi n_1}{l_1}) - 2\cos(-\frac{2\pi n_1 l_3}{l_1 l_4} + \frac{2\pi n_2}{l_4}) \right] . \quad (59)$$

[2019-08-06 Predrag] From this formula it is impossible to see that the answer is an integer, let alone how to compute it. Please state the answer in terms of Chebyshev polynomials in s, as in (26).

[2019-08-06 Predrag] What happened to *shadowing*? One of the main points of this and the companion papers is that periodic orbits shadowing generalizes to invariant 2-tori shadowing in higher spatiotemporal dimensions. Include 2d invariant 2-tori shadowing figures.

In the spirit of section 4.6, we now illustrate the theory by explicitly verifying the periodic-point counting formulas for several 2-dimensional spatiotemporal cat examples. For all our examples we pick the 'least stretching' hyperbolic spatiotemporal cat with $s = 5$, and restrict the admissible field values x_z at lattice site $z = (n_1, n_2)$ to the symmetric unit interval $x \in [-1/2, 1/2)$, with 9-letter alphabet

$$\mathcal{A} = \{\underline{4}, \underline{3}, \underline{2}, \underline{1}, 0, 1, 2, 3, 4\} . \quad (60)$$

[2019-08-11 Predrag] to Han - I might be wrong, are $\mathcal{A} = \{\underline{5}, 5\}$ also to be included?

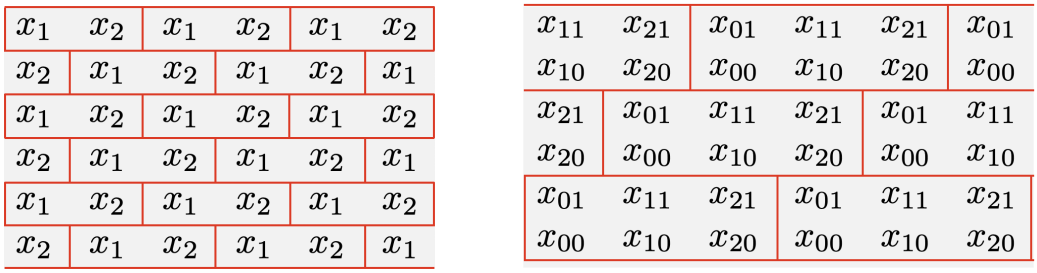

Figure 7. Examples of invariant 2-tori $[L_1 \times L_2]$ together with their spatiotemporal lattice Bravais tilings (52). (a) $[2\times 1]$, basis vectors $\mathbf{a}_1 = \{2,0\}$ and $\mathbf{a}_2 = \{1,1\}$; (b) $[3\times 2]$, basis vectors $\mathbf{a}_1 = (3,0)$ and $\mathbf{a}_2 = (1,2)$. Rectangles enclose the primitive cell, and its Bravais lattice translations.

6.2. An example: Relative $[2\times 1]$ *invariant 2-torus*

Consider a $[2\times 1]$ invariant 2-torus with relative (screw) periodic bc's, periodic state $\mathsf{X}_{m_1 m_2} = \begin{bmatrix} x_1 & x_2 \end{bmatrix}$, tiled by the Bravais lattice (52) with basis vectors $\mathbf{a}_1 = \{2,0\}$ and $\mathbf{a}_2 = \{1,1\}$, see figure 7 (a). This is the simplest example of a spatiotemporal cat tiling that is not just a 1-dimensional temporal cat periodic orbit solution along one direction, repeated along the other.

[2019-08-11 Predrag] to Han - we need something like
For the $s = 5$ example at hand, (59) yields the numbers of relative prime invariant 2-tori $[L_1\times 1]$

$$\{M_{L_1\times 1}\} = (M_{1\times 1}, M_{2\times 1}, M_{3\times 1}, \cdots) = (1, 9, ?, ?, ?, \cdots)\,, \tag{61}$$

to be contrasted with temporal cat counting (21), this time for $s = 5$,

$$\{M_n\} = (M_1, M_2, M_3, M_4, M_5, \cdots) = (1, ?, ?, ?, ?, \cdots)\,. \tag{62}$$

By (59) the number of $[2\times 1]$ invariant 2-tori with the given Bravais lattice bc's is:

$$N_{2\times 1} = \prod_{n_1=0}^{1}\prod_{n_2=0}^{0}\left[s - 2\cos 2\pi\frac{n_1}{2} - 2\cos 2\pi(\frac{n_1}{2} - n_2)\right] = 9\,.$$

Using the Green's function method (38) one can verify that there are indeed 9 such invariant 2-tori, one invariant 2-torus solution for each letter of alphabet (60),

$$\mathsf{X}_{\underline{m}m} = \frac{1}{9}\begin{bmatrix} -m & m \end{bmatrix}\,, \qquad m \in \mathcal{A}\,, \tag{63}$$

for example

$$\mathsf{M} = \begin{bmatrix} -4 & 4 \end{bmatrix} \Rightarrow \quad \mathsf{X}_{\underline{4}4} = \frac{1}{9}\begin{bmatrix} -4 & 4 \end{bmatrix}\,.$$

Note that these are 'periodic point' solutions: the *prime* invariant 2-tori consist of sets of periodic points related by cyclic permutations, $\overline{\underline{m}m} = (\mathsf{X}_{\underline{m}m}, \mathsf{X}_{m\underline{m}})$, and there are only 4 of those, as $\mathsf{X}_{00} = \mathsf{X}_0$ is a repeat of a 1-block.

6.3. An example: Relative $[3 \times 2]$ *invariant 2-torus*

Using the eigenvectors, we can diagonalize the Hessian matrix to find its inverse, i.e., the Green's function. For example, consider a specific invariant 2-torus which has the periodicity given by the Bravais lattice (52) with the basis vectors $\mathbf{a}_1 = (3, 0)$ and $\mathbf{a}_2 = (1, 2)$, as shown in figure 5. The pattern of this solution is shown in figure 7 (b). There are 6 independent field values in the repeating cell, which can be written as an 3×2 array:

$$\begin{bmatrix} x_{01} & x_{11} & x_{21} \\ x_{00} & x_{10} & x_{20} \end{bmatrix} .$$

The corresponding Hessian symmetric (tensor) matrix (42) is a $[3 \times 2] \times [3 \times 2]$ rank-4 tensor. If $s = 5$, the elements of this tensor be H_{i_1,j_1,i_2,j_2}, the Hessian of this periodic pattern are:

[2019-08-07 Predrag] Not sure we want to list this out, but I would prefer (tensor) matrix notation $H_{zz'} = H_{nt,n't'}$

$$\mathsf{X}_z = \sum_{z'}^{L_p T_p} (H^{-1})_{zz'} \mathsf{M}_{z'} .$$

And, why this allergy to names 'Fourier'? 'Toeplitz'? 'Chebyshev'? All the literature I collected for you is to nought? Expression like 'commuting' or 'discrete Fourier transform'? Anyway, concentrate on other part of the paper while I ponder most economical tensorial notation...

$$(-\Box + s - 4)_{0,0,i_2,j_2} = (H_{0,0})_{i_2,j_2} = \begin{bmatrix} -1 & -1 & 0 \\ 5 & -1 & -1 \end{bmatrix}_{i_2,j_2} ,$$

$$(-\Box + s - 4)_{0,1,i_2,j_2} = (H_{0,1})_{i_2,j_2} = \begin{bmatrix} 5 & -1 & -1 \\ -1 & 0 & -1 \end{bmatrix}_{i_2,j_2} ,$$

$$(-\Box + s - 4)_{1,0,i_2,j_2} = (H_{1,0})_{i_2,j_2} = \begin{bmatrix} 0 & -1 & -1 \\ -1 & 5 & -1 \end{bmatrix}_{i_2,j_2} ,$$

$$(-\Box + s - 4)_{1,1,i_2,j_2} = (H_{1,1})_{i_2,j_2} = \begin{bmatrix} -1 & 5 & -1 \\ -1 & -1 & 0 \end{bmatrix}_{i_2,j_2} ,$$

$$(-\Box + s - 4)_{2,0,i_2,j_2} = (H_{2,0})_{i_2,j_2} = \begin{bmatrix} -1 & 0 & -1 \\ -1 & -1 & 5 \end{bmatrix}_{i_2,j_2} ,$$

$$(-\Box + s - 4)_{2,1,i_2,j_2} = (H_{2,1})_{i_2,j_2} = \begin{bmatrix} -1 & -1 & 5 \\ 0 & -1 & -1 \end{bmatrix}_{i_2,j_2} .$$

To diagonalize this rank-4 Hessian we need to use the the eigenvectors (57) to form a rank-4 tensor:

$$U_{i_1,j_1,i_2,j_2} = \exp\left(i \frac{2\pi}{6} (2 i_2 i_1 - i_2 j_1 + 3 j_2 j_1) \right) .$$

The inverse of this tensor is the conjugate transpose $U^\dagger$:

$$(U^\dagger)_{i_1,j_1,i_2,j_2} = (U_{i_2,j_2,i_1,j_1})^* \,.$$

The diagonalized Hessian is:

$$(H_{\text{diagonalized}})_{i_1,j_1,i_2,j_2} = \sum_{i_3=0}^{2}\sum_{j_3=0}^{1}\sum_{i_4=0}^{2}\sum_{j_4=0}^{1}(U^\dagger)_{i_1,j_1,i_3,j_3}H_{i_3,j_3,i_4,j_4}U_{i_4,j_4,i_2,j_2} \,.$$

The diagonalized Hessian's element $(H_{\text{diagonalized}})_{i_1,j_1,i_2,j_2}$ is not 0 only when $i_1 = i_2$ and $j_1 = j_2$. We can get the inverse of this diagonalized tensor, $H^{-1}_{\text{diagonalized}}$, by changing the non-zero elements to their inverse. Then inverse of the Hessian is:

$$(H^{-1})_{i_1,j_1,i_2,j_2} == \sum_{i_3=0}^{2}\sum_{j_3=0}^{1}\sum_{i_4=0}^{2}\sum_{j_4=0}^{1}U_{i_1,j_1,i_3,j_3}(H^{-1}_{\text{diagonalized}})_{i_3,j_3,i_4,j_4}(U^\dagger)_{i_4,j_4,i_2,j_2} \,.$$

The elements of the inverse Hessian are:

$$(H^{-1}_{0,0})_{i_2,j_2} = \frac{1}{35}\begin{bmatrix} 5 & 5 & 4 \\ 11 & 5 & 5 \end{bmatrix}_{i_2,j_2},$$

$$(H^{-1}_{0,1})_{i_2,j_2} = \frac{1}{35}\begin{bmatrix} 11 & 5 & 5 \\ 5 & 4 & 5 \end{bmatrix}_{i_2,j_2},$$

$$(H^{-1}_{1,0})_{i_2,j_2} = \frac{1}{35}\begin{bmatrix} 4 & 5 & 5 \\ 5 & 11 & 5 \end{bmatrix}_{i_2,j_2},$$

$$(H^{-1}_{1,1})_{i_2,j_2} = \frac{1}{35}\begin{bmatrix} 5 & 11 & 5 \\ 5 & 5 & 4 \end{bmatrix}_{i_2,j_2},$$

$$(H^{-1}_{2,0})_{i_2,j_2} = \frac{1}{35}\begin{bmatrix} 5 & 4 & 5 \\ 5 & 5 & 11 \end{bmatrix}_{i_2,j_2},$$

$$(H^{-1}_{2,1})_{i_2,j_2} = \frac{1}{35}\begin{bmatrix} 5 & 5 & 11 \\ 4 & 5 & 5 \end{bmatrix}_{i_2,j_2}.$$

The inverse of the Hessian H^{-1} is the Green's function. For a given admissible source block M, the periodic field can be computed by:

$$\mathsf{X}_{i_1,j_1} = \sum_{i_2=0}^{2}\sum_{j_2=0}^{1}H^{-1}_{i_1,j_1,i_2,j_2}\mathsf{M}_{i_2,j_2} \,.$$

For example, if the source M is:

$$\mathsf{M} = \begin{bmatrix} 0 & 2 & 0 \\ -1 & 0 & 0 \end{bmatrix},$$

the corresponding field is:

$$\mathsf{X} = \begin{bmatrix} x_{01} & x_{11} & x_{21} \\ x_{00} & x_{10} & x_{20} \end{bmatrix} = \frac{1}{35}\begin{bmatrix} 5 & 17 & 6 \\ -1 & 5 & 3 \end{bmatrix}.$$

Substitute this solution into figure 7 (b) we can see that (34) is satisfied everywhere.

7. Summary and discussion

In this paper we have analyzed the spatiotemporal cat (35) linear symbolic dynamics. We now summarize our main findings.

[2016-11-08 Predrag] Say: THE BIG DEAL is
for d-dimensional field theory, symbolic dynamics is not one temporal sequence with a huge alphabet, but d-dimensional spatiotemporal tiling by a finite alphabet
"Classical foundations of many-particle quantum chaos" I believe could become a game-changer
corresponding dynamical zeta functions should be sums over invariant 2-tori, rather than 1-dimensional periodic orbits

[2016-11-01 Boris] **"Deeper insight" into $d = 2$ symbolic dynamics**: Relevance to semiclassics.

[2016-11-10 Predrag] Curb you enthusiasm **How to think about matters spatiotemporal?** text currently purged from the introduction:

Laws of motion drive a spatially extended system (clouds, say) through a repertoire of unstable patterns, each defined over a finite spatiotemporal region.
But in dynamics, we have no fear of the infinite extent in time. That is periodic orbit theory's [31] raison d'être; the dynamics itself describes the infinite time strange sets by a hierarchical succession of periodic orbits, of longer and longer, but always finite periods (with no artificial external periodicity imposed along the time axis). And, since 1996 we know how to deal with both spatially and temporally infinite regions by tiling them with finite spatiotemporally periodic tiles [23, 41]. More precisely: a time periodic orbit is computed in a finite time, with period T, but its repeats "tile" the time axis for all times. Similarly, a spatiotemporally periodic "tile" or "invariant 2-torus" is computed on a finite spatial region L, for a finite period T, but its repeats in both time and space directions tile the infinite spacetime.
Taken together, these open a path to determining exact solutions on *spatially infinite* regions. This is important, as many turbulent flows of physical interest come equipped with D continuous spatial symmetries. For example, in a pipe flow at transitional Reynolds number, the azimuthal and radial directions (measured in viscosity length units) are compact, while the pipe length is infinite. If the theory is recast as a d-dimensional space-time theory, $d = D + 1$, spatiotemporally translational invariant recurrent solutions are invariant d-tori (and *not* the 1-dimensional periodic orbits of the traditional periodic orbit theory), and the symbolic dynamics is likewise d-dimensional (rather than what is today taken for given, a single 1-dimensional temporal string of symbols).
This changes everything. Instead of studying time evolution of a chaotic system, one now studies the repertoire of spatiotemporal patterns allowed by a given PDE. To put it more provocatively: junk your old equations and look for guidance in clouds' repeating patterns. There is no more *time* in this vision of nonlinear *dynamics*! Instead, there is the space of all spatiotemporal patterns, and the likelihood that a given finite spatiotemporally pattern can appear, like the mischievous grin of Cheshire cat, anywhere in the turbulent evolution of a flow. A bold proposal, but

how does it work?

and thus a d-dimensional spatiotemporal pattern is mapped one-to-one onto a d-dimensional discrete lattice state, symbolic dynamics labelled configuration - a configuration very much like that of an Ising model of statistical mechanics.

7.1. Discussion.

[2016-12-24 Predrag] " Alternatively, one can consider the dynamics on the infinite line, and interpret m_t as a jump to m_tth interval. This leads to the phenomenon of "deterministic diffusion" [44, 85], and its periodic orbit theory [7, 29], with unit circle periodic orbits in one-to-one relation to the relative periodic ("running") orbits on the line, and symbolic dynamics given by m_t's.
For single-parameter, 1-dimensional sawtooth maps, it is possible to find infinitely many values of the parameter such that the grammar is finite (a finite subshift), and the exact diffusion constant is given by a finite-polynomial topological zeta function [8]. For cat maps, deterministic diffusion constants are not known exactly [10].
"

Remarkably, as far as the linear symbolic dynamics is concerned, the above results hold both for the single cat map and its coupled lattice generalization. In both cases the proofs rely only upon ellipticity of the operator $\Box$ and the linearity of the equations. It is very plausible that the same results hold for the lattices $\mathbb{Z}^d$ of an arbitrary dimension d. Furthermore, the restriction to the integer valued matrices in the definitions of maps appears unnecessary. Cat map is a smooth version of the sawtooth map, defined by the same equation (11), but for a real (not necessarily integer) value of s. The linear symbolic dynamics for single saw map has been analyzed in [76] and its extension to a coupled $\mathbb{Z}^d$ model along the lines of the present paper seems to be straightforward. Also, in the current paper we sticked to the Laplacian form of $\Box$. Again this seems to be too restrictive and extension to other elliptic operators of higher order should be possible. Such operators are necessarily appear within the models with higher range of interactions.

A physically necessary extension of current setting would be addition of an external periodic potential V to (35), rendering this a nonlinear problem,

$$(\Box - s + 2d + V'(x_z))x_z = m_z, \qquad z \in \mathbb{Z}^d\,. \tag{64}$$

As long as the perturbation V is sufficiently weak, this lattice map can be conjugated to the linear spatiotemporal cat, with $V = 0$. This approach has been used in [47] to construct partner invariant 2-tori for perturbed cat map lattices. On the other hand, for a sufficiently strong perturbation, such a conjugation to linear system is no longer possible. Finally, let us note that the lattice models like (64) can be seen as discretized versions of PDEs. In this respect it would be of interest to study whether our results can be extended to the continuous, PDE setting. In particular, the following questions seem to be of fundamental importance:

- Can an effective $d = 2$ symbolic dynamics with finite alphabet be constructed for an example of a PDE with spatiotemporal chaos, such that (a) Connection between periodic field solutions and their symbolic representation is unique; (b) The local symbolic content would define the values of the corresponding fields with the exponentially decreasing errors?

While the setting is classical, such classical field-theory advances offer new semi-classical approaches to quantum field theory and many-body problems.

Acknowledgments

Work of P. C. was in part supported by the family of late G. Robinson, Jr.. No actual cats, graduate or undergraduate, have shown interest in, or were harmed during this research. This paper sets up the necessary underpinnings for the quantum field theory of spatiotemporal cat, the details of which we leave to our always trustworthy friends Jon Keating and Marcos Saraceno.

Appendix A. Symbolic dynamics: a glossary

Analysis of a low-dimensional chaotic dynamical system typically starts [31] with establishing that a flow is locally stretching, globally folding. The flow is then reduced to a discrete time return map by appropriate Poincaré sections. Its state space is partitioned, the partitions labeled by an alphabet, and the qualitatively distinct solutions classified by their temporal symbol sequences. Thus our analysis of the cat map and the spatiotemporal cat requires recalling and generalising a few standard symbolic dynamics notions.

Partitions, alphabets. A division of state space $\mathcal{M}$ into a disjoint union of distinct regions $\mathcal{M}_A, \mathcal{M}_B, \ldots, \mathcal{M}_Z$ constitutes a *partition*. Label each region by a symbol m from an N-letter *alphabet* $\mathcal{A} = \{A, B, C, \cdots, Z\}$, where $N = n_{\mathcal{A}}$ is the number of such regions. Alternatively, one can distinguish different regions by coloring them, with colors serving as the "letters" of the alphabet. For notational convenience, in alphabets we sometimes denote negative integer m by underlining them, as in $\mathcal{A} = \{-2, -1, 0, 1\} = \{\underline{2}, \underline{1}, 0, 1\}$.

Itineraries. For a dynamical system evolving in time, every state space point $x_0 \in \mathcal{M}$ has the *future itinerary*, an infinite sequence of symbols $S^+(x_0) = m_1 m_2 m_3 \cdots$ which indicates the temporal order in which the regions shall be visited. Given a trajectory $x_1, x_2, x_3, \cdots$ of the initial point x_0 generated by a time-evolution law $x_{n+1} = f(x_n)$, the itinerary is given by the symbol sequence

$$m_n = m \qquad \text{if} \qquad x_n \in \mathcal{M}_m \,. \tag{A.1}$$

The *past itinerary* $S^-(x_0) = \cdots m_{-2} m_{-1} m_0$ describes the order in which the regions were visited up to arriving to the point x_0. Each point x_0 thus has associated with it the

bi-infinite itinerary

$$S(x_0) = S^{\text{-}}.S^{+} = \cdots m_{-2}m_{-1}m_0.m_1m_2m_3\cdots\,, \tag{A.2}$$

or simply 'itinerary', if we chose not to use the decimal point to indicate the present,

$$\{m_t\} = \cdots m_{-2}m_{-1}m_0m_1m_2m_3\cdots \tag{A.3}$$

Shifts. A forward iteration of temporal dynamics $x \to x' = f(x)$ shifts the entire itinerary to the left through the 'decimal point'. This operation, denoted by the shift operator σ,

$$\sigma(\cdots m_{-2}m_{-1}m_0.m_1m_2m_3\cdots) = \cdots m_{-2}m_{-1}m_0m_1.m_2m_3\cdots\,, \tag{A.4}$$

demotes the current partition label m_1 from the future S^{+} to the past $S^{\text{-}}$. The inverse shift σ^{-1} shifts the entire itinerary one step to the right.

The set of all itineraries that can be formed from the letters of the alphabet $\mathcal{A}$ is called the *full shift*

$$\hat{\Sigma} = \{(m_k) : m_k \in \mathcal{A} \quad \text{for all} \quad k \in \mathbb{Z}\}\,. \tag{A.5}$$

The itinerary is infinite for any trapped (non-escaping or non–wandering set orbit) orbit (such as an orbit that stays on a chaotic repeller), and infinitely repeating for a periodic orbit p of period n_p. A map f is said to be a *horseshoe* if its restriction to the non–wandering set is hyperbolic and topologically conjugate to the full $\mathcal{A}$-shift.

Lattices. Consider a d-dimensional hypercubic lattice infinite in extent, with each site labeled by d integers $z \in \mathbb{Z}^d$. Assign to each site z a letter m_z from a finite alphabet $\mathcal{A}$. A particular fixed set of letters m_z corresponds to a particular lattice state $\mathsf{M} = \{m_z\}$. In other words, a d-dimensional lattice requires a d-dimensional code $\mathsf{M} = \{m_{n_1n_2\cdots n_d}\}$ for a complete specification of the corresponding state X. In the lattice case, the *full shift* is the set of all d-dimensional symbol blocks that can be formed from the letters of the alphabet $\mathcal{A}$

$$\hat{\Sigma} = \{\{m_z\} : m_z \in \mathcal{A} \quad \text{for all} \quad z \in \mathbb{Z}^d\}\,. \tag{A.6}$$

Commuting discrete translations. For an autonomous dynamical system, the evolution law f is of the same form for all times. If f is also of the same form at every lattice site, the group of lattice translations (sometimes called multidimensional shifts), acting along jth lattice direction by shift σ_j, is a spatial symmetry that commutes with the temporal evolution. A temporal mapping f that satisfies $f \circ \sigma_j = \sigma_j \circ f$ along the $d-1$ spatial lattice directions is said to be *shift invariant*, with the associated symmetry of dynamics given by the d-dimensional group of discrete spatiotemporal translations.

Assign to each site z a letter m_z from the alphabet $\mathcal{A}$. A particular fixed set of letters m_z corresponds to a particular lattice symbol array $\mathsf{M} = \{m_z\} = \{m_{n_1n_2\cdots n_d}\}$, which yields a complete specification of the corresponding state X. In the lattice case, the *full shift* is the set of all d-dimensional symbol arrays that can be formed from the letters of the alphabet $\mathcal{A}$

as in (A.6)

A d-dimensional spatiotemporal field $\mathsf{X} = \{x_z\}$ is determined by the corresponding *d-dimensional* spatiotemporal symbol array $\mathsf{M} = \{m_z\}$. Consider next a finite block of symbols $\mathsf{M}_\mathcal{R} \subset \mathsf{M}$, over a finite rectangular $[L_1 \times L_2 \times \cdots \times L_d]$ lattice region $\mathcal{R} \subset \mathbb{Z}^d$. In particular, let M_p over a finite rectangular $[L_1 \times L_2 \times \cdots \times L_d]$ lattice region be the $[L_1 \times L_2 \times \cdots \times L_d]$ d-periodic block of M whose repeats tile $\mathbb{Z}^d$.

Blocks. In the case of temporal dynamics, a finite itinerary $\mathsf{M}_\mathcal{R} = m_{k+1} m_{k+2} \cdots m_{k+L}$ of symbols from $\mathcal{A}$ is called a *block* of length $L = n_\mathcal{R}$. More generally, let $\mathcal{R} \subset \mathbb{Z}^d$ be a $[L_1 \times L_2 \times \cdots L_d]$ rectangular lattice region, $L_k \geq 1$, whose lower left corner is the $n = (n_1 n_2 \cdots n_d)$ lattice site

$$\mathcal{R} = \mathcal{R}_n^{[L_1 \times L_2 \times \cdots L_d]} = \{(n_1 + j_1, \cdots n_d + j_d) \mid 0 \leq j_k \leq L_k - 1\} \,. \tag{A.7}$$

The associated finite block of symbols $m_z \in \mathcal{A}$ restricted to $\mathcal{R}$, $\mathsf{M}_\mathcal{R} = \{m_z | z \in \mathcal{R}\} \subset \mathsf{M}$ is called the block $\mathsf{M}_\mathcal{R}$ of volume $n_\mathcal{R} = L_1 L_2 \cdots L_d$. For example, for a 2-dimensional lattice a $\mathcal{R} = [3 \times 2]$ block is of form

$$\mathsf{M}_\mathcal{R} = \begin{bmatrix} m_{12} & m_{22} & m_{32} \\ m_{11} & m_{21} & m_{31} \end{bmatrix} \tag{A.8}$$

and volume (in this case, an area) equals $3 \times 2 = 6$. In our convention, the first index is 'space', increasing from left to right, and the second index is 'time', increasing from bottom up.

Cylinder sets. While a particular admissible infinite symbol array $\mathsf{M} = \{m_z\}$ defines a point X (a unique lattice state) in the state space, the *cylinder set* $\mathcal{M}_{\mathsf{M}_\mathcal{R}}$, corresponds to the totality of state space points X that share the same given finite block $\mathsf{M}_\mathcal{R}$ symbolic representation over the region $\mathcal{R}$. For example, in $d = 1$ case

$$\mathcal{M}_{\mathsf{M}_\mathcal{R}} = \{\cdots a_{-2} a_{-1} \,.\, m_1 m_2 \cdots m_L a_{L+1} a_{L+2} \cdots\} \,, \tag{A.9}$$

with the symbols a_j outside of the block $\mathsf{M}_\mathcal{R} = [m_1 m_2 \cdots m_L]$ unspecified.

Periodic orbits, invariant d-tori. A state space point $x_z \in \mathsf{X}$ is spatiotemporally *periodic*, $x_z = x_{z+L}$, if its spacetime orbit returns to it after a finite lattice shift $L = (L_1, L_2, \cdots, L_d)$ over region $\mathcal{R}$ defined in (A.7). The infinity of repeats of the corresponding block $\mathsf{M}_\mathcal{R}$ then tiles the lattice. For a spatiotemporally periodic state X, a *prime* block M_p (or p) is a smallest such block $L_p = (L_1, L_2, \cdots, L_d)$ that cannot itself be tiled by repeats of a shorter block.

The periodic tiling of the lattice by the infinitely many repeats of a prime block is denoted by a bar: $\overline{\mathsf{M}}_p$. We shall omit the bar whenever it is clear from the context that the state is periodic.

[2019-01-19 Predrag] eliminate $\_m_{-m+1} \cdots m_0\_$ and $[m_{-m+1} \cdots m_0 .,]$ notation in favor a single convention

[2018-11-07 Predrag] Generalize to invariant d-tori.

In $d = 1$ dimensions, prime block is called a *prime* cycle p, or a single traversal of the orbit; its label is a block of n_p symbols that cannot be written as a repeat of a

shorter block. Each *periodic point* $x_{m_1 m_2 \cdots m_{n_p}}$ is then labeled by the starting symbol m_1, followed by the next $(n_p - 1)$ steps of its future itinerary. The set of periodic points $\mathcal{M}_p$ that belong to a given periodic orbit form a *cycle*

$$p = \overline{m_1 m_2 \cdots m_{n_p}} = \{x_{m_1 m_2 \cdots m_{n_p}}, x_{m_2 \cdots m_{n_p} m_1}, \cdots, x_{m_{n_p} m_1 \cdots m_{n_p - 1}}\} . \quad \text{(A.10)}$$

More generally, a state space point is *spatiotemporally periodic* if it belongs to an invariant d-torus, i.e., its symbolic representation is a block over region $\mathcal{R}$ defined by (A.7),

$$\mathsf{M}_p = \mathsf{M}_{\mathcal{R}} , \qquad \mathcal{R} = \mathcal{R}_0^{[L_1 \times L_2 \times \cdots \times L_d]} , \quad \text{(A.11)}$$

that tiles the lattice state M periodically, with period L_j in the jth lattice direction.

Generating partitions. A temporal partition is called *generating* if every bi-infinite itinerary corresponds to a distinct point in state space. In practice almost any generating partition of interest is infinite. Even when the dynamics assigns a unique infinite itinerary $\cdots m_{-2} m_{-1} m_0 . m_1 m_2 m_3 \cdots$ to each distinct orbit, there generically exist full shift itineraries (A.5) which are not realized as orbits; such sequences are called *inadmissible*, and we say that the symbolic dynamics is *pruned*.

Dynamical partitions. If the symbols outside of given temporal block b remain unspecified, the set of all admissible blocks of length n_b yield a dynamically generated partition of the state space, $\mathcal{M} = \cup_b \mathcal{M}_b$.

Subshifts. A dynamical system $(\mathcal{M}, f)$ given by a mapping $f : \mathcal{M} \to \mathcal{M}$ together with a partition $\mathcal{A}$ induces *topological dynamics* (Σ, σ), where the *subshift*

$$\Sigma = \{(m_k)_{k \in \mathbb{Z}}\} , \quad \text{(A.12)}$$

is the set of all *admissible* itineraries, and $\sigma : \Sigma \to \Sigma$ is the shift operator (A.4). The designation 'subshift' comes from the fact that Σ is the subset of the full shift.

Let $\hat{\Sigma}$ be the full lattice shift (A.5), i.e., the set of all possible lattice state M labelings by the alphabet $\mathcal{A}$, and $\hat{\Sigma}(\mathsf{M}_{\mathcal{R}})$ is the set of such blocks over a region $\mathcal{R}$. The principal task in developing the symbolic dynamics of a dynamical system is to determine Σ, the set of all *admissible* itineraries/lattice states, i.e., all states that can be realized by the given system.

Pruning, grammars, recoding. If certain states are inadmissible, the alphabet must be supplemented by a *grammar*, a set of pruning rules. Suppose that the grammar can be stated as a finite number of pruning rules, each forbidding a block of finite size,

$$\mathcal{G} = \{b_1, b_2, \cdots b_k\} , \quad \text{(A.13)}$$

where a *pruned block* b is an array of symbols defined over a finite $\mathcal{R}$ lattice region of size $[L_1 \times L_2 \times \cdots \times L_d]$. In this case we can construct a finite Markov partition by replacing finite size blocks of the original partition by letters of a new alphabet. In the case of a 1-dimensional, the temporal lattice, if the longest forbidden block is of length $L + 1$, we say that the symbolic dynamics is Markov, a shift of finite type with L-step memory.

Subshifts of finite type. A topological dynamical system (Σ, σ) for which all admissible states M are generated by recursive application of the finite set of pruning rules (A.13) is called a subshift of *finite type*.

If a map can be topologically conjugated to a linear map, the symbolic dynamics of the linear map offers a dramatically simplified description of all admissible solutions of the original flow, with the temporal symbolic dynamics and the state space dynamics related by linear recoding formulas. For example, if a map of an interval, such as a parabola, can be conjugated to a piecewise linear map, the kneading theory [74] classifies *all* of its admissible orbits. Cat maps are linear, but there are several ways of taking advantage of their linearity.

References

Appendix B. Hill's formula

Appendix B.1. Generating functions; action

[2016-11-11, 2018-09-26 Predrag] What follows is (initially) copied from Li and Tomsovic [65], *Exact relations between homoclinic and periodic orbit actions in chaotic systems* arXiv source file, then merged with the MacKay-Meiss-Percival action principle [69, 71].

For discrete-time one-degree-of-freedom Lagrangian systems satisfying a periodicity condition (i.e., cat map):

$$L(q+1, q'+1) = L(q, q') + C\,, \tag{B.1}$$

one can consider relative periodic paths (or pre-periodic paths, also called periodic paths of type (ℓ, n) by Mackay and Meiss [68]), with

[2018-09-29 Predrag] presumably they are relative periodic orbits, or pre-periodic orbits, with a rational winding number p/q.

$$q_{i+n} = q_i + \ell\,. \tag{B.2}$$

Every q_i returns to its value after time period n, but shifted by ℓ. Orbits satisfying (B.2) are given by stationary points of the action

$$W = \sum_{i=0}^{q-1} L(q_i, q_{i+1}) \tag{B.3}$$

in the space of periodic paths of type (ℓ, n). For periodic paths, it suffices to consider one period, because an orbit is periodic if and only if it is a stationary point of the action of one period in the space of periodic paths.

If the constant C (the Calabi invariant [21]) in the periodicity condition (B.1) is zero, and the Lagrangian satisfies a convexity condition

$$L_{12}(q,q') < 0\,, \tag{B.4}$$

where subscript k refers to the derivative with respect to the kth argument, then the action of periodic paths of type (ℓ, n) is bounded below, so there is a minimising path. Since its action is stationary, it gives a periodic orbit of type (ℓ, n).

[2018-01-21 Predrag] Is this true? To go from the Hamiltonian (x_t, p_t) phase space formulation to the Newtonian (or Lagrangian) (x_{t-1}, x_t) *state space* formulation, replace p_t by $p_t = (x_t - x_{t-1})/\Delta t$, where $\Delta t = 1$.

For prime periodic orbit p of period n_p, the action of the orbit is:

$$W_p \equiv \sum_{n=0}^{n_p-1} L(q_n, q_{n+1})\ . \tag{B.5}$$

W_p is the generating function that maps a point along the orbit for one (prime) period. For the case of a fixed point p of period $n_p = 1$, the action is

$$W_p = L(q_p, q_p)\,, \tag{B.6}$$

where the generating function $L(q_p, q_p)$ maps x_p into itself in one iteration.

Appendix C. Homoclinic and periodic orbit actions in chaotic systems

[2018-09-29 Predrag] What follows is copied from Li and Tomsovic [65].

For an aperiodic orbit $\{x_0\}$ going through the point x_0, the action, evaluated as the sum over an infinity of successive mappings,

$$W_{\{x_0\}} \equiv \lim_{N\to\infty} \sum_{n=-N}^{N-1} L(q_n, q_{n+1}) = \lim_{N\to\infty} W_{-N,N}\,, \tag{C.1}$$

is not necessarily convergent. However, the MacKay-Meiss-Percival action principle [69, 71] can be applied to obtain well defined action differences between pairs of orbits. For example, the *relative action* $\Delta W_{\{h_0\}\{x\}}$ between a fixed point x_p and its homoclinic orbit $\{h_0\}$, where $h_{\pm\infty} \to x_p$:

$$\begin{aligned}
\Delta W_{\{h_0\}\{x_p\}} &\equiv \lim_{N\to\infty} \sum_{i=-N}^{N-1} [L(h_i, h_{i+1}) - L(x_p, x_p)] \\
&= \int_{U[x_p,h_0]} p\mathrm{d}q + \int_{S[h_0,x_p]} p\mathrm{d}q = \oint_{US[x_p,h_0]} p\mathrm{d}q \\
&= \mathcal{A}^{\circ}_{US[x_p,h_0]}
\end{aligned} \tag{C.2}$$

where $U[x_p, h_0]$ is the segment of the unstable manifold from x_p to h_0, and $S[h_0, x_p]$ the segment of the stable manifold from h_0 to x_p. The $\circ$ superscript on the last line

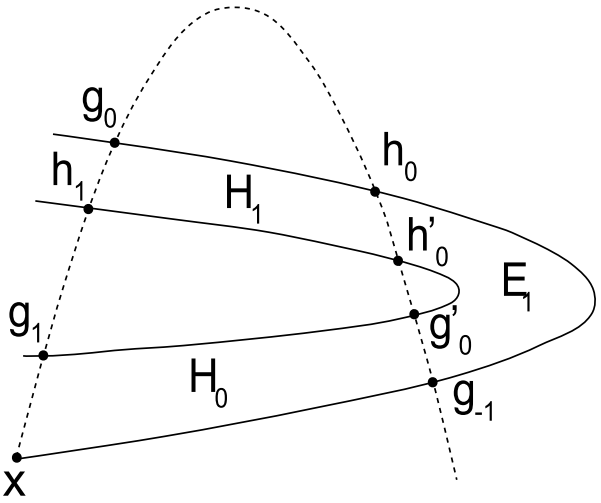

Figure C1. A sketch of a partial homoclinic tangle which forms a complete horseshoe structure. The unstable (stable) manifold of x is the solid (dashed) curve. There are two primary homoclinic orbits $\{h_0\}$ and $\{g_0\}$. $\mathcal{R}$ is the closed region bounded by loop $\mathcal{L}_{USUS[x,g_{-1},h_0,g_0]}$. (From [65])

indicates that the area is interior to a path that forms a closed loop, and the subscript indicates the path: $US[x_p, h_0] = U[x_p, h_0] + S[h_0, x_p]$. The clockwise enclosure of an area is positive, counterclockwise negative. $\Delta W_{\{h_0\}\{x_p\}}$ gives the action difference between the homoclinic orbit segment $[h_{-N}, \cdots, h_N]$ and the length-$(2N+1)$ fixed point orbit segment $[x_p, \cdots, x_p]$ in the limit $N \to \infty$. In later sections, upon specifying the symbolic code of the homoclinic orbit $\{h_0\} \Rightarrow \overline{0}\gamma\overline{0}$, we also denote $\Delta W_{\{h_0\}\{x_p\}}$ alternatively as

$$\Delta W_{\{h_0\}\{x_p\}} = \Delta W_{\overline{0}\gamma\overline{0},\overline{0}} \tag{C.3}$$

by replacing the orbits in the subscript with their symbolic codes.

Likewise, a second important case is for the relative action between a pair of homoclinic orbits $\{h'_0\} \Rightarrow \overline{0}\gamma'\overline{0}$ and $\{h_0\} \Rightarrow \overline{0}\gamma\overline{0}$, which results in

$$\begin{aligned}
\Delta W_{\{h'_0\}\{h_0\}} &\equiv \lim_{N\to\infty} \sum_{i=-N}^{N-1} \left[L(h'_i, h'_{i+1}) - L(h_i, h_{i+1})\right] \\
&= \lim_{N\to\infty} \left[L(h'_{-N}, h'_N) - L(h_{-N}, h_N)\right] \\
&= \int_{U[h_0,h'_0]} p\mathrm{d}q + \int_{S[h'_0,h_0]} p\mathrm{d}q = \mathcal{A}^{\circ}_{US[h_0,h'_0]} \\
&= \Delta W_{\overline{0}\gamma'\overline{0},\overline{0}\gamma\overline{0}}
\end{aligned} \tag{C.4}$$

where $U[h_0, h'_0]$ is the segment of the unstable manifold from h_0 to h'_0, and $S[h'_0, h_0]$ the segment of the stable manifold from h'_0 to h_0. Due to the fact that the endpoints approach x_p forward and backward in time, one can also write

$$\begin{aligned}
\Delta W_{\{h'_0\}\{h_0\}} = &\lim_{N\to\infty} \left[L(h'_{-(N+n)}, h'_{N+m}) - L(h_{-N}, h_N)\right] \\
&- (n+m)\mathcal{F}_0\,.
\end{aligned} \tag{C.5}$$

Appendix D. Hill's formula

[2016-11-11, 2018-09-26 Predrag] The current draft of this section starts out with excerpts from Mackay and Meiss [68] *Linear stability of periodic orbits in Lagrangian systems*, and Bolotin and Treschev [17] *Hill's formula*.

There can be more than one minimising path. In particular, translating one minimising path by an integer in time or space or both gives another. This implies existence of saddle points of the action in between the minima, with one downward direction [1-3]. They are called minimax points, and give rise to minimax periodic orbits of type (d, n). The statement of the existence of at least two periodic orbits of each type (d, n) is known as the Poincaré-Birkhoff theorem.

As a corollary, Mackay and Meiss [68] rederive the old result that when the convexity condition is satisfied, the multipliers of a minimising orbit are a reciprocal pair of positive reals, and those of a minimax orbit are either a complex conjugate pair on the unit circle, or a reciprocal pair of negative reals. The result for minimising orbits was shown by Poincaré [81] for two-degree-of-freedom continuous-time systems, and Birkhoff [1] discusses the minimax case.

The linear stability of a periodic orbit is determined by its multipliers, the eigenvalues of the derivative of the return map round the orbit. While the first variation of the action is by definition zero for an orbit, the multipliers of a periodic orbit can be related to the second variations of the action in the space of periodic paths. This has been shown in various cases. Hill [49] and Poincaré [81] derived a formula for the multipliers in the case of one-degree-of-freedom systems of the form kinetic minus potential [49], using a Fourier representation for periodic paths. In his study of periodic orbits of the three-body problem, Hill obtained a formula connecting the characteristic polynomial of the monodromy matrix of a periodic orbit with the infinite determinant of the Hessian of the action functional. Mackay and Meiss [68] derived a formula (D.6) for the multipliers of a periodic orbit for general discrete-time one-degree-of-freedom systems. Bolotin and Treschev [17] give two multidimensional generalizations of Hill's formula: for discrete Lagrangian systems (symplectic twist maps) and for continuous Lagrangian systems, and discuss implications of symmetries and reversibility. Bountis and Helleman [18] and Greene [43] treated the case of discrete-time one-degree-of-freedom systems with

$$L_{12}(q, q') = -1\,. \tag{D.1}$$

Schmidt [86] determined n-tupling bifurcations by the criterion that the matrix of second variations of the action with respect to periodic paths of n times the period have a zero eigenvalue.

Mackay and Meiss [68] relate the multipliers of a periodic orbit to the second variations of the action about the orbit, and compute the determinant of the matrix of second variations of the action in the space of periodic paths of period T.

Stationarity (**??**) of the action for an orbit of a discrete-time one-degree-of-freedom system implies that

$$L_2(q_{i-1}, q_i) + L_1(q_i, q_{i+1}) = 0\,. \tag{D.2}$$

Thus the tangent orbits δx_i satisfy [...]. The multipliers Λ of a periodic orbit of period q are defined by existence of a tangent orbit satisfying [...] residue of a periodic orbit one can easily solve for multipliers. [... losing steam]

Mackay and Meiss [68] formulas for the multipliers of minimising and minimax orbits follow. Under the convexity condition (B.4), the denominator is positive. At a minimum of action (whether local or global):

$$D(1) \leq 0\,, \tag{D.3}$$

so the multipliers are real and positive. At a minimax with one downward direction:

$$D(1) \geq 0\,, \tag{D.4}$$

so the multipliers are on the unit circle or the negative real axis.

Residue [43] R of a periodic orbit p of period n_p

$$4R = \det(\mathbf{1} - J_p) = \mathrm{tr}(\mathbf{1} - J_p) = 2 - \Lambda_p - 1/\Lambda_p \tag{D.5}$$

is related to the determinant $D(\Lambda)$ by what the discrete Hill's formula [17]:

[2018-09-30 Predrag] See Bolotin and Treschev [17] eqs. (2.8) and (2.13)

$$\det(\mathbf{1} - J_p) = -D(1) \left(\prod_{i=0}^{n_p-1} (-L_{12}[i, i+1]) \right)^{-1} . \tag{D.6}$$

This formula was derived by Mackay and Meiss [68] and Allroth [3] (Allroth eq. (12)). It applies to general "one-degree-of-freedom" systems, i.e., 1D lattices with only the nearest neighbor interactions. For a finite set of neighbors, i.e., higher-dimensional discrete-time systems, Allroth [3] has some partial results in the context of Frenkel-Kontorova models.

$D(1)$ is the determinant of the matrix of second variations of the action in the space of periodic paths of period q. So we have related the multipliers of a periodic orbit to the second variations of the action about the orbit.

Appendix F. Kittens' CL18blog

Internal discussions of [28] edits: Move good text not used in [28] to this file, for possible reuse later.

Tentative title: "Is there anything cats cannot do?"

2016-11-18 Predrag A theory of turbulence that has done away with *dynamics*? We rest our case.

2016-10-05 Predrag My approach is that this is written for field theorists, fluid dynamicists etc., who do not see any reason to look at cat maps, so I am trying to be pedagogical, motivate it as that chaotic counterpart of the harmonic oscillator, something that field theorists fell comfortable with (they should not, but they do).

2016-11-13 Predrag The next thing to rethink: Green's functions for periodic lattices are in ChaosBook sections D.3 Lattice derivatives and on, for the Hermitian Laplacian and $s = 2$. For real $s > 2$ cat map, the potential is inverted harmonic oscillator, the frequency is imaginary (Schrödinger in imaginary time), eigenvectors real - should be a straightforward generalization. Have done this already while studying Ornstein-Uhlenbeck with Lippolis and Henninger - the eigenfunctions are Hermite polynomials times Gaussians.

2016-11-13 Predrag Potential inserts, varied temptations

B. Fernandez and P. Guiraud [36]
B. Fernandez and M. Jiang [37]
W. Just [53, 54]

the cat map is linear and the trivial trajectory located at the origin can be regarded as distinguished

2016-11-13 Predrag We write (11) screened Poisson equation as

$$(\Box + 2 - s)x_t = m_t\,, \tag{6.1}$$

Percival and Vivaldi [76] write their Eq. (3.6)

$$(\Box + 2 - s)x_t = -b_t \tag{6.2}$$

so their "stabilising impulses" b_t (defined on interval $x \in [-1/2, 1/2)$) have the opposite sign to our "winding numbers" m_t (defined on $x \in [0, 1)$).
Did not replace Arnol'd by PerViv choice.

$$A = \begin{pmatrix} 0 & 1 \\ -1 & s \end{pmatrix}\,, \tag{6.3}$$

$$\begin{aligned} x_{t+1} &= p_t \mod 1 \\ p_{t+1} &= -x_t + s\,p_t \mod 1 \end{aligned} \tag{6.4}$$

Predrag's formula, removed by Boris 2017-01-15:

$$\begin{aligned} x_{t+1} &= (s-1)\,x_t + p_t \\ p_{t+1} &= (s-2)\,x_t + p_t \end{aligned} \quad \mod 1\,, \tag{6.5}$$

Predrag's formula, removed by Boris 2017-01-15:
As the 3-point discretization of the second time derivative d^2/dt^2 (central difference operator) is $\Box\, x_t \equiv x_{t+1} - 2x_t + x_{t-1}$ (with the time step set to $\Delta t = 1$), the *temporal* cat map (6.11) can be rewritten as the discrete time Newton equation for inverted harmonic potential,

$$(\Box + 2 - s)\, x_t = m_t\,. \tag{6.6}$$

a d-dimensional spatiotemporal pattern $\{x_z\} = \{x_{n_1 n_2 \cdots n_d}\}$ requires *d-dimensional* spatiotemporal block $\{m_z\} = \{m_{n_1 n_2 \cdots n_d}\}$,

2016-08-20 Predrag " The fact that even Dyson [35] counts cat map periods should give us pause - clearly, some nontrivial number theory is afoot. "
Not sure whether this is related to cat map symbolic dynamics that we use, dropped for now: " Problems with the discretization of Arnol'd cat map were pointed out in [15, 16]. [15] discusses two partitions of the cat map unit square. "
" and resist the siren song of the Hecke operators [62, 73] "

2016-05-21 Predrag Behrends [12, 13] *The ghosts of the cat* is fun - he uncovers various regular patterns in the iterates of the cat map.

2016-09-27 Boris Cat maps and spatiotemporal cats
In the spatiotemporal cat, "particles" (i.e., a cat map at each periodic lattice site) are coupled by the next-neighbor coupling rules:

$$q_{n,t+1} = p_{nt} + (s-1)q_{nt} - q_{n+1,t} - q_{n-1,t} - m^q_{n,t+1}$$

$$p_{n,t+1} = p_{nt} + (s-2)q_{nt} - q_{n+1,t} - q_{n-1,t} - m^p_{n,t+1}$$

The symbols of interest can be found by:

$$m_{nt} = q_{n,t+1} + q_{n,t-1} + q_{n+1,t} + q_{n-1,t} - s\, q_{nt}\,.$$

2016-10-27 Boris Gutkin and Osipov [47] write: "In general, calculating periodic orbits of a non-integrable system is a non-trivial task. To this end a number of methods have been developed," and then, for a mysterious reasons, they refer to [11].

2016-10-27 Boris Added to section 6 the following references: M. Sieber and K. Richter [87], S. Müller, S. Heusler, P. Braun, F. Haake and A. Altland [75], Gutkin and Osipov [46], Gutkin and Osipov [45] (Predrag added [47] as well).

2016-11-07 Predrag The dynamical systems literature tends to focus on *local* problems: bifurcations of a single time-invariant solution (equilibrium, relative equilibrium, periodic orbit or relative periodic orbit) in low-dimensional settings (3-5 coupled ODEs, 1-dimensional PDE). The problem that we face is *global*: organizing and relating *simultaneously* infinities of unstable relative periodic orbits

in ∞-dimensional
state spaces, orbits that are presumed to form the skeleton of turbulence (see [40] for a gentle introduction) and are typically not solutions that possess the symmetries of the problem. In this quest we found the standard equivariant bifurcation theory literature not very helpful, as its general focus is on bifurcations of solutions, which admit all or some of the symmetries of the problem at hand.

> [2016-11-15 Predrag] **Homework for all cats**: Write the correct (**??**) for an n-cycle. For inspiration: check ChaosBook.org discussion of the kneading theory, where such formula is written down for unimodal maps. Might require thinking.
> Hint: the answer is in the paper:)

2016-11-17 Boris Unlike the systems studied in [20], spatiotemporal cat cannot be conjugated to a product of non-interacting cat maps; a way to see that is to compare the numbers of periodic orbits in the two cases – they differ.

2016-11-17 Predrag a simple generalization of a Bernoulli map to a Hamiltonian setting
finite grammars whenever all partition borders map onto partition borders.
If one neglects the width of the stretched-out area, get sawtooth maps, with infinity of finite grammars.

The cat map partitions the phase space into $|\mathcal{A}|$ regions, with borders defined by the condition that the two adjacent labels $k, k+1$ simultaneously satisfy (11),

$$x_1 - sx_0 + x_{-1} - \epsilon = k\,, \tag{6.7}$$

$$x_1 - sx_0 + x_{-1} + \epsilon = k+1\,, \tag{6.8}$$

$$x_2 - sx_1 + x_0 = m_1\,, \tag{6.9}$$

$$x_1 - sx_0 + x_{-1} = m_0\,, \tag{6.10}$$

$$(x_0, x_1) = (0,0) \to (0,0)\,, \quad (1,0) \to (0,-1)\,, \quad (0,1) \to (1,s)\,, \quad (1,1) \to (1,s-1)$$

2016-11-05 Predrag Dropped this:
Note the two symmetries of the dynamics [58]: The calculations generalize directly to any cat map invariant under time reversal [60].

2016-11-11 Boris "Deeper insight" into $d = 2$ symbolic dynamics Information comes locally (both in space and time). Allows to understand correlations between invariant 2-tori. Connection with field theories.

2016-12-12 Predrag Predrag text, recycle: " Here the piecewise linearity of the spatiotemporal cat enables us to go far analytically. Essentially, as the cat map stretching is uniform, distinct admissible symbol blocks count all blocks of a given shape (they all have the same stability, and thus the same dynamical weight), and that can be accomplished by linear, Green's function methods. "

2017-08-28 Predrag "Average state" depends on bc's. Average state GHJSC16.tex eq. catMapAverCoord is computed for the very unphysical Dirichlet bc's $x_z = 0$ for $z \in \mathcal{R}$ which breaks translation invariance. If one takes the much gentler, translationally invariant doubly periodic b.c., the "average state" $\bar{x}_z$ is the invariant 2-torus periodic point, a more natural choice.

2017-08-28 Predrag Probably lots of repeats with existing text:
Consider a linear, area preserving map of a 2-torus onto itself

[2019-10-31 Predrag] compare with (3)

$$\begin{pmatrix} x_{t+1} \\ p_{t+1} \end{pmatrix} = A \begin{pmatrix} x_t \\ p_t \end{pmatrix} \mod 1\,, \qquad A = \begin{pmatrix} s-1 & 1 \\ s-2 & 1 \end{pmatrix}\,, \tag{6.11}$$

where both x_t and p_t belong to the unit interval. For integer $s = \mathrm{tr}\, A > 2$ the map is referred to as a cat map [5]. It is a fully chaotic Hamiltonian dynamical system, which, rewritten as a 2-step difference equation in (x_t, x_{t-1}) takes a particularly simple form (8) with a unique integer "winding number" m_t at every time step t ensuring that x_{t+1} lands in the unit interval [76]. While the dynamics is linear, the nonlinearity comes through the (mod 1) operation, encoded in $m_t \in \mathcal{A}$, where $\mathcal{A}$ is finite alphabet of possible values for m_t.

A generalization to the *spatiotemporal* cat map is now immediate. Consider a 1-dimensional spatial lattice, with field $x_{n,t}$ (the angle of a kicked rotor "particle" at instant t) at site n. If each site couples only to its nearest neighbors $x_{n\pm1,t}$, and if we require (1) invariance under spatial translations, (2) invariance under spatial reflections, and (3) invariance under the space-time exchange, we arrive at the 2-dimensional Euclidean cat map lattice (34). Note that both equations (8), (34) can be brought into uniform notation and generalized to d dimensions by converting the spatialtemporal differences to discrete derivatives. This yields the Newton (or Lagrange) equation for the d-dimensional *spatiotemporal cat* (35) where $\Box$ is the discrete d-dimensional Euclidean space-time Laplacian, given by $\Box\, x_t \equiv x_{t+1} - 2x_t + x_{t-1}$, $\Box x_{n,t+1} \equiv x_{n,t+1} + x_{n,t-1} - 4\, x_{n,t} + x_{n+1,t} + x_{n-1,t}$ in $d = 1$ and $d = 2$ dimensions, respectively. The key insight (an insight that applies to all coupled-map lattices, and all PDEs modeled by them, not only the system considered here) is that a d-dimensional spatiotemporal pattern $\{x_z\} = \{x_z, z \in \mathbb{Z}^d\}$ is described by the corresponding *d-dimensional* spatiotemporal symbols block $\{m_z\} = \{m_z, z \in \mathbb{Z}^d\}$, rather than a *single* temporal symbol sequence (as one is tempted to do when describing a finite coupled N^{d-1}-"particle" system).

the cat map in one dimension (temporal dynamics of a single "particle") and for the spatiotemporal cat (35) in d dimensions (temporal dynamics of a (d-1)-dimensional spatial lattice of N^{d-1} interacting "particles," $N \to \infty$). Linearity of (35) enables us to solve for $\{x_z\}$ given $\{m_z\}$ by lattice Green's function methods. However, dependence on the parameter s introduces an infinite set of grammar rules for admissible itineraries $\{m_z\}$. In this paper we focus on the $d = 1$ case (introduced in [76]), and the $d = 2$ case (introduced in [47]).

2018-11-16 Predrag some potential verbiage for abstract, introduction:

Recent advances in fluid dynamics reveal that the recurrent patterns observed in turbulent flows result from close passes to unstable invariant solutions of Navier-Stokes equations. While hundreds of such solutions been computed, they are always confined to small computational domains, while the flows of interest (pipe, channel, plane flows), are flows on infinite spatial domains. To describe them, we recast the Navier-Stokes equations as a spacetime theory, with all infinite translational directions treated on equal footing.

We illustrate this by solving what is arguably the simplest classical field theory, the discretized screened Poisson equation, or the "spatiotemporal cat", and describe its repertoire of admissible spatiotemporal patterns. We encode these by spatiotemporal symbol dynamics (rather than a single temporal string of symbols). In the spatiotemporal formulation of turbulence there are no periodic orbits, as there is no time evolution. Instead, the theory is formulated in terms of unstable spacetime tori, which are minimal tilings of spacetime. The measure concept here is akin to the statistical mechanics understanding of the Ising model - what is the likelihood of occurrence of a given spacetime configuration?

Herding cats

No actual cats, graduate or undergraduate, have shown interest in, or were harmed during this research.

In the spatiotemporal formulation of turbulence the zeta functions (Fredholm determinants) are presumably 2-d or (1+3)-d Laplace/Fourier transforms of trace formulas, one dimension for each continuous symmetry: one Laplace transform for time, and one Fourier transform for each infinite spatial direction.

We have not written either the trace or the determinant formulas yet. The spatiotemporal cat periodic points (invariant 2-tori) counting suggests a way, so far unexplored.

We sketch how these are to be encoded by spatiotemporal symbol dynamics, in terms of minimal exact coherent structures. To determine these, radically different kinds of codes will have to be written, with space and time treated on equal footing.

- review cat map in damped Poisson formulation
- explain solution for temporal cat
- show few plots of 2D solutions
- future: computational literature that advocates for spatiotemporal computations

2019-05-20 Han My action of cat map is different from Keating's action [59] by two constant terms, which do not affect the computation.

2019-05-23 Han I rewrote the section of Perron-Frobenius operators and periodic orbits theory of cat maps and moved the original version here.

2018-02-16 Predrag Dropped this: " , both for the cat map (8) in one dimension (temporal dynamics of a single "particle") and for the spatiotemporal cat (35) in

d dimensions (temporal dynamics of a (d-1)-dimensional spatial lattice of N^{d-1} interacting "particles," $N \to \infty$). Given a set of $\{m_z\}$, the linearity of (35) enables us to find solution for $\{x_t\}$ by lattice Green's function methods.

However, for our purposes, Adler-Weiss codes still have one fatal shortcoming, and are therefore not used in this paper: for L coupled cat maps the size of the alphabet $|\mathcal{A}|$ (the number of partitions of the phase space, a $2L$-dimensional unit hypercube) grows exponentially with L.

2019-08-10 Predrag .

$$N_n = |\det(A^n - \mathbf{I})| = |\operatorname{tr}(A^n) \; - \; 2\;| = |\Lambda^n + \Lambda^{-n} - \; 2\;|\,, \tag{6.12}$$

if , or

$$N_n = |\operatorname{tr}(A^n)| = |\Lambda^n + \Lambda^{-n}|\,, \tag{6.13}$$

if $\det(A^n) = -1$. Here Λ is the larger eigenvalue (4) of A.

2018-12-01 Predrag Give reference for (6.13). I see it nowhere in Isola [52] or Keating [59].

2019-06-06 Han I cannot find (6.13) either, but it can be proved by explicitly computing the determinant.

2019-05-23 Han Removed the Green's function of periodic bc's part because it is not used in the counting formula. And eventually we will use the Fourier transform to compute the Green's function of periodic bc's instead of the method of finding the general Green's function then applying the periodic bc's, which already failed in 2-dimensional spatiotemporal cat.

[2018-12-03 Han] Here we should use absolute value of the determinant. For cat map this determinant will be negative.

[2018-12-03 Han] I'm not sure what is the reference of the determinant of the Hessian. We get the determinant (**??**) by using Fourier transform to diagonalize the matrix. I haven't seen any article calculated the Hessian of the cat map before.

The Hessian matrix H_n is given by (17).

Hill's formula here is the discrete Hill's formula [17, 68] (D.6). For our problem, $-L_{12}[i, i+1] = 1$.

In practice one can supply only symbol sequences of finite length, in which case the truncated (12) returns a finite trajectory x_t, with a finite accuracy. However, a periodic orbit p of period n (an n-cycle) is infinite in duration, but specified by a finite admissible block $p = [m_1 m_2 \cdots m_n]$. To generate all admissible n-cycles for a given n, list all prime symbol sequences $[m_1 m_2, \cdots m_n]$, (one string per its n cyclic permutations, not composed from repeats of a shorter cycle), apply (12) with cyclic $[n \times n]$ $g_{tt'}$, and then apply modulus one to all points in the cycle,

$$x_t = \sum_{t'=t}^{n+t-1} g_{tt'} m_{t'} \mod 1\,. \tag{6.14}$$

If the cycle is admissible, mod 1 does not affect it. If it is inadmissible, add the string to the list of pruned symbol strings. One can even start with any random sequence $[m_1 m_2 \cdots m_n]$, have mod 1 corral back the stray x_t's into the unit interval, and in this way map any inadmissible symbol sequence into an admissible trajectory of the same duration.

[2018-12-03 Predrag] Mixing $m_{t'}$ and mod 1 strikes me as profoundly wrong.

2016-11-15 Predrag Homework for all cats: Write the correct (6.14) for an n-cycle. For inspiration: check ChaosBook.org discussion of the kneading theory, where such formula is written down for unimodal maps. Might require thinking. Hint: the answer is *this* paper :)

2019-06-10 Han Currently the argument of [28] (this paper) is organized as:

(i) Hamiltonian cat map
(ii) Periodic orbits theory of cat maps
(iii) Lagrangian cat map
(iv) Spatiotemporal cat (Predrag: I call it simply spatiotemporal cat, as it is not a "map")

In the section of Hamiltonian cat map we also introduced the Adler-Weiss generating partition and used the Markov diagram of this partition to compute the topological zeta function.

We need to introduce of Lagrangian cat map before the discussion of the periodic orbits theory. Although we can also get the Lagrangian cat map (**??**) from the linear code (11), we still need to write down the Lagrangian explicitly to define the Hessian matrix, $(H_n)_{ij} = \partial^2 L(\boldsymbol{x})/\partial x_i \partial x_j$. Then we can use the Hill's formula to show that the two counting methods are equivalent.

2019-06-25 Han I added sections 6 and 6.1.

Section 6 *Invariant tori in d-dimensional spatiotemporal cat* introduces the method of finding eigenmodes in d-dimensional spatiotemporal cat.

Section 6.1 *Counting invariant 2-tori* gives the eigenmodes and counting formula of the 2-dimensional spatiotemporal cat in detail as an example.

I also wrote *catMapLatt.tex*, refsect s:2DcatCounting *Counting invariant 2-tori*, which is an alternative version that starts from 2D cat map without giving the formula of general d-dimensional spatiotemporal cat. I feel this is less clear than starting with the d-dimensional spatiotemporal cat, but it follows directly from the section on temporal cat.

2019-08-13 Predrag *catMapLatt.tex* was an experimental, alternative version of section 6 that starts from $d = 2$ cat map without giving the formula of general d-dimensional spatiotemporal cat. Now kept only in blogCats.tex.

2019-08-04 Predrag Note configuration part of the map (1) differs from Percival-Vivaldi [76] (2.1). However, it agrees with MacKay, Meiss and Percival [69] definition (3.4), and Meiss [71] (no discussion of cat maps) definition of the standard map (1.36).

2019-08-04 Predrag Percival-Vivaldi [76] get (8) immediately, their (2.2) for any force from their Hamiltonian (2.1), rather than our Hamiltonian of form (2).

2019-08-01 Han I changed the letter of action (16) from L to W, which is the same letter as in [69, 71]. L is the generating function, and W is the sum of L.
PC 2019-8-03 Yes, but check defsKittens.tex. W has been defined your way since 07jan2018.

2019-08-05 Predrag Rewrite (**??**) as:

$$\begin{aligned} q_{t+1} &= q_t + p_t + (s-2)q_t - {m_{t+1}}^q \\ p_{t+1} &= p_t + (s-2)q_t - {m_{t+1}}^q - ({m_{t+1}}^p - {m_{t+1}}^q)\,. \end{aligned} \tag{6.15}$$

Comparing this with the Hamiltonian mapping (1,2) we identify the impulse $F(q_t)$

$$\begin{aligned} q_{t+1} &= q_t + p_{t+1} \\ p_{t+1} &= p_t + (s-2)q_t - {m_{t+1}}^p\,. \end{aligned} \tag{6.16}$$

where the ${m_{t+1}}^q$ seems happily absorbed into p_{t+1}. The generating function (1-step Lagrangian density) is

2019-05-16 Han For the cat map, the problem of solving for a periodic string eventually becomes solving the linear equation (**??**) for x's. For any set of integers $\boldsymbol{m}$, there is a solution $\boldsymbol{x}$. But the solution is admissible only when each one of the field values in $\boldsymbol{x}$ is larger or equal to 0 and smaller than 1.

2019-05-16 Han Will need to change the range of x_z to $-1/2 \le x_z < 1/2$ if we add the shadowing to this paper.

2019-08-06 Predrag We shall refer here to the least unstable of the cat maps (3), with $s = 3$, as the 'Arnol'd', or 'Arnol'd-Sinai cat map' [5, 32].

2019-05-27 Predrag I see no (23) in Percival and Vivaldi [76, 77] or Isola [52] - papers preceding Keating [59], though it is implicit in Isola [52] eq. (11).

2019-06-06 Han The method of using the determinant $\det(A^n - \mathbf{I})$ to count periodic points is given by Keating [59] eq.(28) and the following paragraph.

2019-07-08 Predrag to Han - you wrote "the equation of motion of d-dimensional cat map." (1) this is no equation of motion; (2) we use "d-dimensional spatiotemporal cat" or screened Poisson equation macro.

2017-01-25 Predrag Do not remember where it came from, but it sure looks worng: Action of an invariant 2-torus p is

$$S_p = -\frac{1}{2}\sum_{t=1}^{T}\sum_{n=1}^{L} m_{nt}x_{nt} \tag{6.17}$$

Still, why the '-' sign?

2017-09-01 Predrag Boris wrote "g is an element of dihedral group D_4". Sure it is the order eight D_4, and not the order four D_2? Write out the list of group elements $\mathrm{D}_8 = \{e, \cdots\}$.

2017-09-15 Boris The measures of the following blocks are equal by D_4 symmetry, see the example in [48], following (**??**).

2019-08-06 Predrag For a discrete Euclidean space-time the Laplacian is given by

$$\Box x_t \equiv x_{t+1} - 2\,x_t + x_{t-1} \tag{6.18}$$

$$\Box x_{nt} \equiv x_{n,t+1} + x_{n+1,t} - 4\,x_{nt} + x_{n,t-1} + x_{n-1,t} \tag{6.19}$$

in $d = 1$ and 2 dimensions, respectively.

2018-02-09 Predrag If I understood his remark correctly, Howie Weiss suggested that we read and cite Weiss-Bowen paper. But I cannot find such paper anywhere where?

2019-08-04 Predrag By MacKay, Meiss and Percival [69, 71] convention (3.2), and Li and Tomsovic [65] convention (9) we should always have $L(q_t, q_{t+1})$. Unfortunately Keating [59] definition (3) corresponds to $L(q_t, q_{t-1})$, but we do not take that one.

2019-08-05 Predrag Not sure we need generating functions, etc. So confine (**??**)-(**??**) to their appendix, or ignore them in this paper altogether.

2019-08-08 Han We derived generating function because the Hessian is defined by the second order partial derivatives of the generating function, $(H)_{ij} = \partial^2 L(\boldsymbol{x})/\partial x_i \partial x_j$. This concept is used in the Hill's formula (28) [17]. I think it's fine to keep that in the appendix.

2019-08-08 Han In examples of section 6.3 and section 6.2 I used the symmetric $x \in [-1/2, 1/2)$ field range of values. And the shadowing that we did before is also in the symmetric domain. I can change them back to the asymmetric $x \in [0, 1)$ domain if needed, since in section 5 the alphabet (35) is asymmetric.

2018-08-08 Han I have been trying to write the counting formula (59) in a concise form since last year, but haven't reached any success... Not even with the simplest regular periodic condition ($l_3 = 0$ in (55)) (see our blog (**??**–**??**)). A good thing about (59) is that when the basis vectors have a symmetric form in (55), for example, $l_3 = 0$, the counting formula becomes:

$$N = \prod_{n_1=0}^{l_1-1} \prod_{n_2=0}^{l_4-1} \left[s - 2\cos(\frac{2\pi n_1}{l_1}) - 2\cos(\frac{2\pi n_2}{l_4}) \right]. \tag{6.20}$$

The number of invariant 2-tori is unchanged under the exchange of spatial length and temporal length of the block. Anyway, I'm still checking the references in Green2d.tex, trying to make this formula prettier.

2019-08-10 Predrag I find figure 1 very helpful in giving us a visual understanding of what a Hamiltonian cat map does, and how the periodic orbit counting comes about. Can you draw the corresponding Percival-Vivaldi representation fundamental parallelogram (22) for $s = 3$, $n = 2$ or $n = 3$, let's say? to visualize how (21) comes about.

2019-08-08 Han Invariant 2-tori (63) written out:

$$\mathsf{X}_{\underline{33}} = \frac{1}{9}\begin{bmatrix} -3 & 3 \end{bmatrix}, \quad \mathsf{X}_{\underline{22}} = \frac{1}{9}\begin{bmatrix} -2 & 2 \end{bmatrix}, \quad \mathsf{X}_{\underline{11}} = \frac{1}{9}\begin{bmatrix} -1 & 1 \end{bmatrix},$$

$$\mathsf{X}_{00} = \frac{1}{9}\begin{bmatrix} 0 & 0 \end{bmatrix}, \quad \mathsf{X}_{1\underline{1}} = \frac{1}{9}\begin{bmatrix} 1 & -1 \end{bmatrix}, \quad \mathsf{X}_{2\underline{2}} = \frac{1}{9}\begin{bmatrix} 2 & -2 \end{bmatrix},$$
$$\mathsf{X}_{3\underline{3}} = \frac{1}{9}\begin{bmatrix} 3 & -3 \end{bmatrix}, \quad \mathsf{X}_{4\underline{4}} = \frac{1}{9}\begin{bmatrix} 4 & -4 \end{bmatrix}. \tag{6.21}$$

2019-08-10 Predrag The example of figure 7 is a very important, great you are writing it up. One recurring remark how to make such formulas shorter, in the spirit of (31):

$$\mathsf{X}_{4\underline{4}} = \frac{1}{9}\begin{bmatrix} 4 & -4 \end{bmatrix}, \tag{6.22}$$

use M array as a subscript of the periodic state X, (the label for prime orbit p) instead of (6.21).

2019-08-11 Predrag Can one visualize the *fundamental parallelogram* (22) for $s = 3$, $n = 2$ (or $n = 3$)? Formula (23) is so hard to *explain* to anyone. The real triumph would be a figure that explains the Hessian (25) and (one has a right to dream!) the Hill's formula (29).

2019-08-12 Han I have figures in the blog tried to visualize the Hessian (25). The figures and the post are moved here. We can only visualize this for $n \leq 3$. A longer period can only be shown in higher dimensional space. The two figures in figure F1 are made with asymmetric admissible domain $x \in [0, 1)$. If these two figures are helpful I can redo these using the symmetric domain $x \in [-1/2, 1/2)$.

2019-01-08 Han I made figure F1 to show how the volume (area) of the stretched torus counts the number of periodic points. Consider the cat map with $s = 3$. The periodic solutions satisfy:

$$H_n \mathbf{x} = \mathbf{m}\,, \tag{6.23}$$

where H_n is the Hessian of the periodic orbit with period n. If any $\mathbf{x}$ on the torus satisfies (6.23), this $\mathbf{x}$ is a periodic solution. So we can count the periodic points using H_n to stretch the torus and counting the number of integer points enclosed in the stretched region. I plotted the stretched region of periodic solutions with $n = 2$ and $n = 3$. The Hessians for $n = 2$ and $n = 3$ are:

$$H_2 = \begin{pmatrix} 3 & -2 \\ -2 & 3 \end{pmatrix} \tag{6.24}$$

$$H_3 = \begin{pmatrix} 3 & -1 & -1 \\ -1 & 3 & -1 \\ -1 & -1 & 3 \end{pmatrix} \tag{6.25}$$

Let the range of the field value x be $0 \leq x < 1$. Figure F1 (a) shows the number of periodic points with length 2. The unit square enclosed by black lines is the available region of (x_n, x_{n+1}). The parallelogram with red borders are the region of the unit square stretched by the Hessian H_2. There are 4 blue dots which are the integer points in the parallelogram. Each one of these blue dots corresponds to a periodic

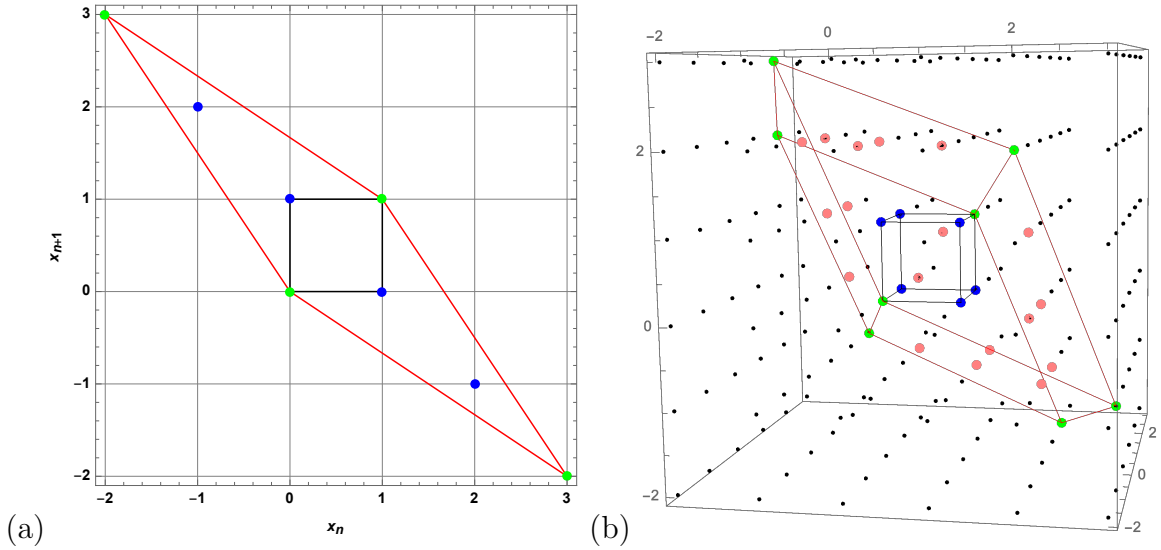

Figure F1. (a) A 2-dimensional torus (with black border) stretched by H_2. The blue dots are internal integer points in the stretched parallelogram (with red border). The green dots are on the vertices of the parallelogram. (b) A 3-dimensional torus (with black border) stretched by H_3. The blue dots are internal integer points in the stretched parallelepiped (with red border). The green dots are on the vertices of the parallelepiped. The pink dots are on the surface of the parallelepiped.

point. The 4 green dots are integer points on the vertices of the parallelogram. These 4 points contribute to 1 periodic point. So there are 5 periodic points with period 2, corresponding to 3 periodic solutions (1 fixed point and 2 2-cycles). The area of this parallelogram is 5.

Figure F1 (b) shows the periodic points with length 3. The square cube with black border is the available region of torus (x_n, x_{n+1}, x_{n+2}). After stretched by Hessian H_3 it becomes the parallelepiped with red border. There are 6 blue dots which are the integer points completely enclosed in the parallelepiped. The 8 green dots are integer points on the vertices of the parallelepiped, which contribute to 1 periodic points. There are 18 pink points which are integer points on the surface of the parallelepiped. These 18 points contribute to 9 periodic points. So the number of periodic points is 16 which is also the volume of the parallelepiped. I have a Mathematica notebook with this 3d plot in siminos/figSrc/han/Mathematica /HLCountingFigures.nb so you can rotate it.

2019-08-13 Predrag I am starting to worry that you have not only forgotten point groups (39) from our group theory course, but also the discrete Fourier transforms? How do you prove formulas such as (26)? Are you sticking the formula into Mathematica? The product of eigenvalues of H,

$$N_n = \det H = \prod_{j=0}^{n-1} \left[s - 2\cos\left(\frac{2\pi j}{n}\right) \right] , \tag{6.26}$$

goes over all eigenfunctions $\exp 2\pi j/n$, so one presumably uses the orthonormality

of discrete Fourier eigenmodes in replacing cos's by a polynomial in s.
Is that how you are trying to simplify (6.20)?

2019-08-13 Han I get (26) by calculating the determinant of the circulant Hessian matrix directly (basically a recurrence relation). I haven't figured out how to get the Chebyshev polynomial using the orthonormality of discrete Fourier eigenmodes...

2019-08-13 Predrag I remember this funky argument from your blog (right?), was never a fan. If you just copied that to here with on further edits, we can erase it again.
Try substituting (6.26) into topological zeta function (24), see whether there are some doable sums over discrete Fourier eigenvalues $\exp 2\pi jk/n$?

2019-08-21 Han I redid the shadowing plot in a larger $[18 \times 18]$ block with $s = 5$. The algorithm is same as before:
(1) Start with a random admissible state X^0 with $-1/2 \le x_z < 1/2$. Calculate the corresponding symbol block M^0. The m_zs in this symbol block are not integers. So we need to round these m_zs to the nearest integers and get symbol block M^1
(2) Use the Green's function and the integer symbol block M^1 to calculate the state X^1. If the maximum x_{max} is larger or equal to $1/2$, calculate the distance $\delta x_{max} = x_{max} - 1/2$. Round up $s\delta x_{max}$ (and call it δm_{max}). Then change the corresponding symbol m_{max} to $m_{max} - \delta m_{max}$. If the minimum x_{min} is smaller than $1/2$, calculate the distance $\delta x_{min} = -x_{min} - 1/2$. Round up $s\delta x_{min}$ (and call it δm_{min}). Then change the corresponding symbol m_{min} to $m_{min} + \delta m_{min}$.
(3) Now we get a new symbol block M^2. Repeat step (2) until all x_z in X are in the admissible range.
Using this method we get two periodic blocks of symbols shown in figure F2. In these two blocks of symbols the m_z within the $[12 \times 12]$ square region with black borders are the same. The periodic field generated by these two blocks of symbol are shown in figure F3. Figure F4 shows the pointwise distance and the logarithm of the absolute value of the pointwise distance between the two invariant 2-tori in figure F3.

2019-08-21 Han I also did the shadowing plot of $[18 \times 18]$ blocks with a smaller shared region of symbols. As shown in figures F5 and F6, the shared region is a $[8 \times 8]$ block.
What I'm considering is: the symbols are on invariant 2-tori, so as we go further from the center of the shared region, we are getting closer to the shared region of the next tile. Using a smaller shared region we can probably reduce the effect of the next shared region. But compare figure F4 (b) and figure F7 (b), the logarithm of the distance is not too different. So I guess we don't need these figures with small shared region...
Also I think this exponential shadowing only exist in the region with shared symbols? In figure F4 (b) and figure F7 (b), the distance outside of the shared region looks random, while the distance within the shared region shrink exponentially as

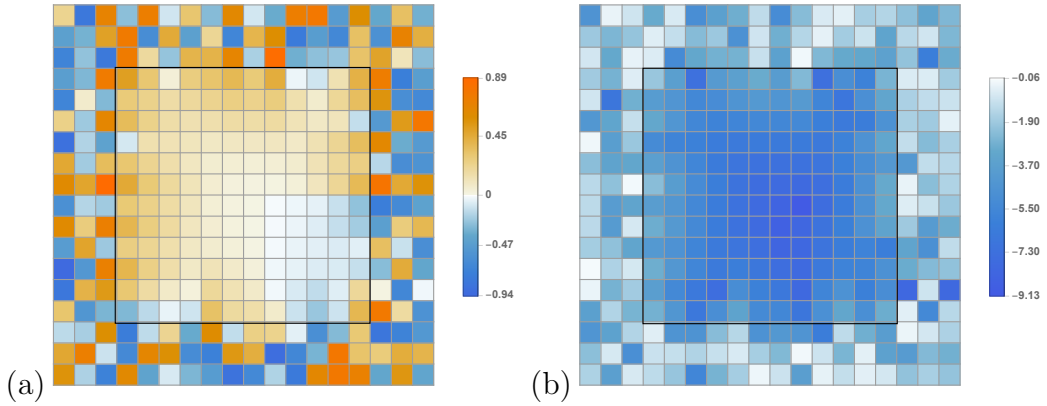

Figure F4. (a) The pointwise distance between the two invariant 2-tori of figure F3. (b) The logarithm of the absolute value of the distance between the two invariant 2-tori indicate exponential shadowing close to the center of the shared $\mathsf{M}_{\mathcal{R}}$.

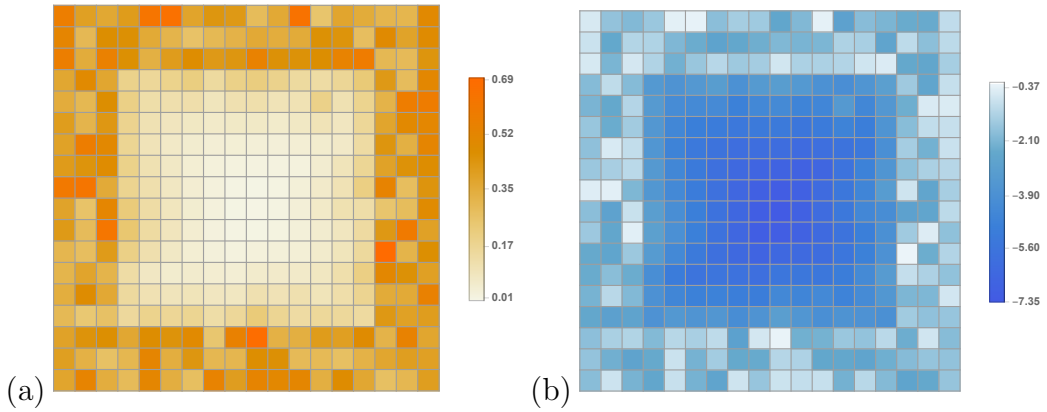

Figure F8. (a) The average of the absolute value of the pointwise distance between the one invariant 2-torus and other 10 different invariant 2-tori with shared $[12 \times 12]$ block of symbols. (b) The logarithm of the average of the absolute value of the distance between the invariant 2-tori indicate exponential shadowing close to the center of the shared $\mathsf{M}_{\mathcal{R}}$.

2019-08-21 Han Another thing I tried is to generate 11 different $[18 \times 18]$ invariant 2-tori shared a same $[12 \times 12]$ block of symbols. Take one of these invariant 2-tori and compute the distance between this invariant 2-torus and other 10 invariant 2-tori, then compute the ensemble average. The result is shown in figure F8, which looks very similar to figure F4. Perhaps using a larger group of ensemble we can get a better result?

2019-08-22 Han I generated 500 different invariant 2-tori with a shared $[12\times12]$ block of symbols at the center, labeled as $\mathsf{X}_1, \mathsf{X}_2, \ldots, \mathsf{X}_{500}$. Then I compute the distance between X_i and X_{i+250} where i goes from 1 to 250, and get 250 distance field. Figure F9 is the log plot of the absolute value of the distance field. Figure F9 (a) is the logarithm of the distance between field X_1 and X_{251}, and (b) is the the logarithm of the average of the 250 distance field. By doing the average, the distance field becomes smooth. Figure F10 is the cross section of figure F9 through the center of the field. In figure F10 (b) the logarithm of the distance is straight line in the region with shared symbols, which shows that the distance shrink exponentially as getting closer to the center.

In figure F10 (b), the logarithm of the distance outside of the shared symbol block is approximately equal to $\ln(1/3) = -1.0986$, where $1/3$ is the average distance between two random numbers within the range $[-1/2, 1/2)$.

I still need to add axis labels to these figures... (It seems like Mathematica doesn't allow me to use LaTeX for writing the labels.)

2019-09-05 Predrag dropped this: $(x \mapsto Ax \,|\, x \in \mathbb{T}^2 = \mathbb{R}^2/\mathbb{Z}^2 \,;\; A \in SL(2,\mathbb{Z}))$,
on no time-forward map,

In **??** we derive the Lagrangian formulation of cat maps.

Cat map is so simple that going from Hamiltonian to Lagrangian formulation

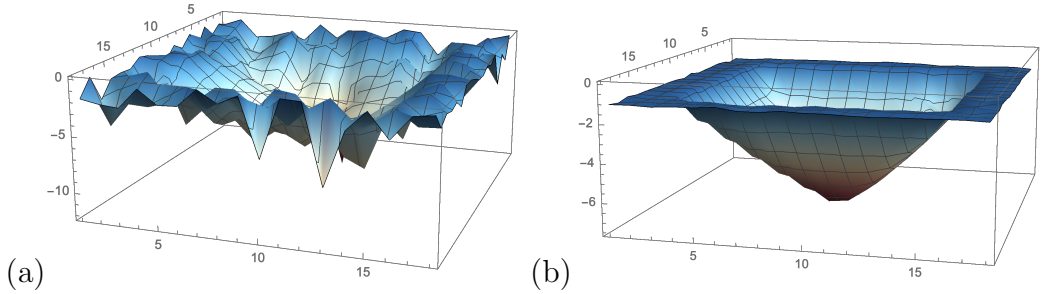

Figure F9. (a) The logarithm of the absolute value of the pointwise distance between the solutions X_1 and X_{251} with shared $[12 \times 12]$ block of symbols at the center. (b) The logarithm of the average of the absolute value of 250 different distance fields.

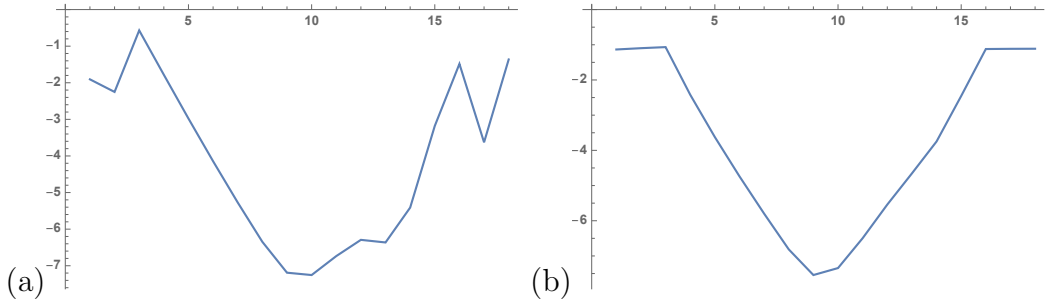

Figure F10. (a) The cross section through the center of the figure F9 (a). (b) The cross section through the center of the figure F9 (b). The logarithm of the distance decreases linearly as the coordinate of the field approaches the center of the shared symbol block.

amounts to replacement (5) of momentum by velocity. Still, for what follows, it might pay off to understand the general theory of transformations from discrete Hamiltonians to discrete Lagrangians; we review that in **??**.

Note to Predrag - send this paper to Vladimir Rosenhaus vladr@kitp.ucsb.edu